Technische Universität München, Fakultät für Medizin

Interrogating the Involvement of Non-classical Monocytes in Early Pancreatic Cancer Metastasis

Xiaopeng Zhang

Vollständiger Abdruck der von der Fakultät für Medizin der Technische Universität München zur Erlangung des akademischen Grades eines

Doktors der Medizin (Dr. med.)

genehmigten Dissertation.

Vorsitz: Prof. Dr. Gabriele Multhoff

Prüfende/-r der Dissertation:

1. Prof. Dr. Radu Roland Rad
2. Prof. Dr. Marc Schmidt-Supprian

Die Dissertation wurde am 15.11.2021 der Technische Universität München eingereicht und durch die Fakultät für Medizin 07.06.2022 angenommen.

Für meine Frau Zijun Cindy Zheng und meine Eltern

To my wife Zijun Cindy Zheng and my parents

Abbreviations

53631m	53631 mock shRNA stable transfected cell line
53631pkd	53631 Padi4 shRNA stable transtected cell line
Ang-1	Angiopoietin-1
Ang-2	Angiopoietin-2
BSA	Bovine serum albumin
BM	Bone marrow
Ca^{2+}	Calcium
CAFs	Cancer-associated fibroblasts
CCR2	C-C chemokine receptor 2
DMSO	Dimethylsulfoxid
DNA	Deoxyribonucleic acid
EVs	Extracellular vesicles
IM	Inflammatory monocyte
LSM	Laser scanning microscope
LOs	Large oncosomes
MV	Micro-vesicles
Mus	Musculus, Mouse
nMs/NM	Non-classical monocytes
NR4A1	Nerve growth factor IB
Padi4	Peptidyl Arginine Deiminase 4
PAI1	Plasminogen activator inhibitor 1
PBS	Phosphate buffered saline
PDAC	Pancreatic ductal adenocarcinoma
RNA	Ribonecleic acid
TFPI	Tissue Factor Pathway Inhibitor
VEGF	Vascular endothelial growth factor
WB	Western Blotting
WT	Wild type

Summary

Pancreatic ductal adenocarcinoma (PDAC) is one of the most lethal malignancies with a high mortality-to-prevalence ratio and exhibits the strongest association with activation of blood coagulation among all carcinomas. In the present study, immunohistochemistry was used to analyze immune cell recruitment to the site of metastasis upon tail vein injection of two PDAC cell lines in mice and. Recruitment of non-classical monocytes (nMs) was highly associated with procoagulant activities of these two cell lines. Moreover, this fibrin-mediated recruitment of nMs was dependent on the integrin CD11b. The recruitment of non-classical monocytes was associated with reduced tumor cell extravasation at the site of metastasis in experiments using cell line 8182. In contrast, non-classical monocytes were linked to increased extravasation of cell line 53631. The latter line released large amounts of extracellular vesicles (EVs). EVs can induce expression of angiopoietin-2 by non-classical monocytes, which might counteract the inhibitory effect of non-classical monocytes on cancer cell extravasation. Thus, nMs might play a dual role in PDAC extravasation: nMs might hinder tumour cell extravasation when tumour EVs are absent, but facilitate cancer cell extravasation when EVs are present. This hypothesis needs evaluation in larger experimental series.

Zusammenfassung

Das duktale Adenokarzinom der Bauchspeicheldrüse (PDAC) ist eine der tödlichsten Malignome. Sie hat ein hohes Mortalitäts-zu-Prävalenz-Verhältnis und weist unter allen Karzinomen die stärkste Assoziation mit der Aktivierung der Blutgerinnung auf. In der vorliegenden Studie wurde mit Hilfe der Immunhistochemie die Rekrutierung von Immunzellen an den Ort der Metastasierung im Rahmen der Injektion von zwei PDAC-Zelllinien in die Schwanzvene von Mäusen analysiert. Die Rekrutierung von nicht-klassischen Monozyten (nMs) war in hohem Maße mit der prokoagulatorischen Aktivität dieser beiden Zelllinien verbunden. Darüber hinaus war diese Fibrin-vermittelte Rekrutierung von nMs von dem Integrin CD11b abhängig. Die Rekrutierung von nicht-klassischen Monozyten war in Experimenten mit der Zelllinie 8182 mit einer verringerten Extravasation von Tumorzellen am Ort der Metastasierung verbunden. Im Gegensatz dazu waren bei der Zelllinie 53631 nicht-klassische Monozyten mit einer verstärkten Extravasation assoziiert. Die letztgenannte Linie setzte große Mengen an extrazellulären Vesikeln (EVs) frei. EVs können die Expression von Angiopoietin-2 durch nicht-klassische Monozyten induzieren, was der hemmenden Wirkung von nicht-klassischen Monozyten auf die Extravasation von Krebszellen entgegenwirken könnte. Somit könnten nMs eine doppelte Rolle bei der PDAC-Extravasation spielen: nMs könnten die Extravasation von Tumorzellen hemmen, wenn keine Tumor-EVs vorhanden sind, jedoch die Extravasation von Krebszellen erleichtern, wenn EVs vorhanden sind. Diese Hypothese muss in größeren Versuchsreihen evaluiert werden.

Table of Contents

1. Introduction

1.1 Pancreatic cancer

1.1.1 Overview of pancreatic cancer

Pancreatic ductal adenocarcinoma (PDAC) accounts for over 90% of pancreatic cancers and is recognized as one of the cancer types with the poorest prognosis (Disease, Injury et al. 2016, Pishvaian and Brody 2017). Regarding morbidity in North America in 2020, pancreatic cancer was the tenth most common cancer in males and the ninth in females. However, pancreatic cancer possessed the highest mortality-to-incidence ratio and led to 47,050 cancer deaths in 57,600 diagnosed cases in 2020, making it the third leading cause of overall cancer-related death (Collaborators 2019, Siegel, Miller et al. 2020). Due to a lack of specific clinical manifestations, over 85% of patients were diagnosed with either metastatic lesions or locally advanced tumors that were unresectable with current surgical techniques when they first visited an oncologist. The median survival time of these patients is 12 months and no more than 3% of them can survive over 5 years (Ducreux, Boige et al. 2007, Ryan, Hong et al. 2014, Neoptolemos, Kleeff et al. 2018). Surgical tumor removal is currently the only method for conquering this fatal disease. Since no promising official therapeutic strategy has been discovered in the past 10 years, the epidemiologists in both Europe and the United States have predicted that pancreatic cancer will become the second most common cause of tumor-related death in the coming 10 years (Rahib, Smith et al. 2014, Ryan, Hong et al. 2014, Are, Chowdhury et al. 2016).

An epidemiological survey validated several factors that increase pancreatic cancer risk, such as age, ethnicity, tobacco and alcohol consumption, excess weight, glycometabolism disorders, exposure to some chemicals, sex, and chronic pancreatitis (Smith, Andrews et al. 2019). Even though pancreatic cancer tends to be a silent killer, there are some limited

diagnostic clues. Abdominal pain and weight loss are the most common symptoms, which are unfortunately nonspecific. The remaining symptoms are mostly dependent on the tumor location. Lesions located in the head of the pancreas tend to induce obstructive jaundice, whereas tumors in the body and tail elicit the sudden occurrence of diabetes due to the destruction of the pancreatic endocrine system (Miller, Nogueira et al. 2019). As both symptoms are nonspecific and there is no biomarker for the early diagnosis of pancreatic cancer, surgical interventions are possible only in rare cases.

1.1.2 Kras mutation in pancreatic cancer

Ras genes are named after **Ra**t **s**arcoma to commemorate the work that identified a cancer-causing virus in rats in the 1960s in the United States (Harvey 1964, Malumbres and Barbacid 2003). Ras genes encode Ras proteins, which are mainly involved in transmembrane cell signal transduction. They are small GTPases and function as an off/on switch for cellular signals. When Ras proteins are switched on, their downstream genes are activated inside the cell nuclei. These downstream gene effectors are responsible for cell proliferation, differentiation, and survival in harsh extracellular conditions. Mutations in Ras genes can permanently activate Ras proteins and their downstream genes, resulting in continuous cell growth and, thereafter, the development of malignancy (Goodsell 1999). Such mutations in Ras genes are widely detected in human carcinomas. The most commonly mutated genes in human are Kras, Hras, and Nras. In pancreatic carcinoma, Kras mutation is the predominant mutation. This mutation is found in more than 80% of pancreatic cancer patients regardless of the cancer stage, and according to some studies, poorer prognoses can potentially be attributed to higher doses of Kras mutation (Downward 2003, Mueller, Engleitner et al. 2018, Buscail, Bournet et al. 2020).

To date, the mechanisms of Kas signaling remain partially enigmatic. Three main pathways are of vital importance. These are Raf/Mek/Erk, PI3K/Pdk1/Akt, and the Ral guanine nucleotide exchange factor pathway (Figure 1) (Lim, Baines et al. 2005, Feldmann, Mishra et al. 2010, Collisson, Trejo et al. 2012, Eser, Reiff et al. 2013).

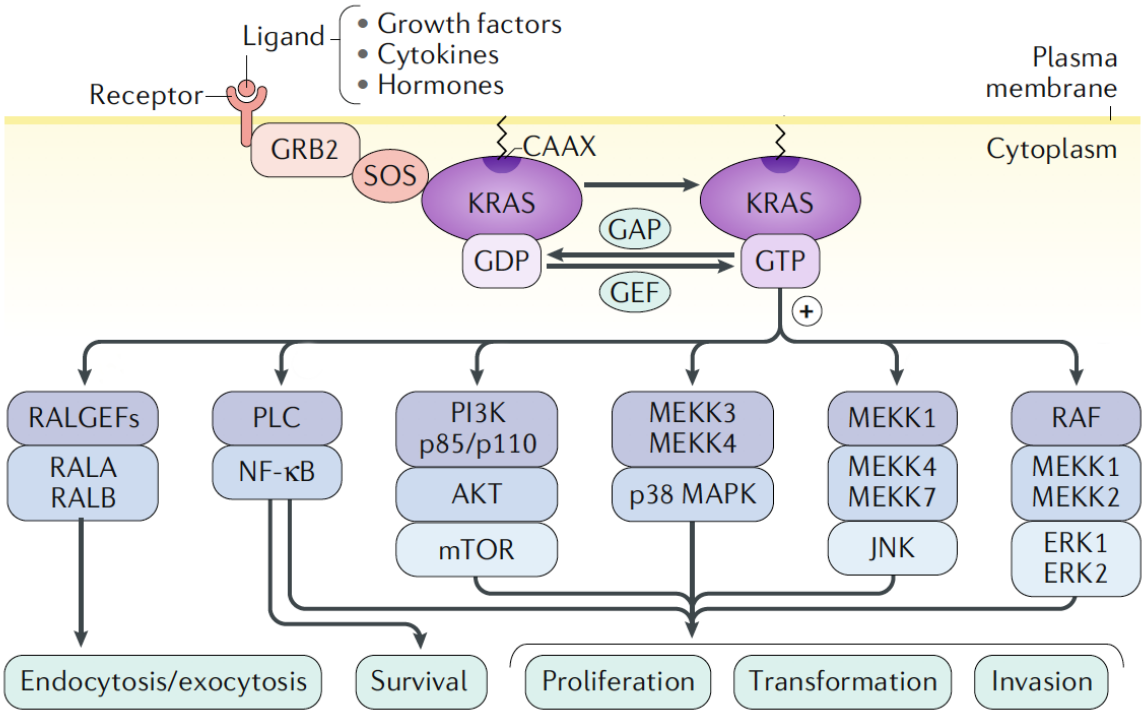

Figure 1 Important downstream effectors of the KRAS signaling pathway. See Ref (Buscail, Bournet et al. 2020)

The tumorigenic functions of Kras are amplified by numerous cross-signaling circuits via known autocrine and paracrine mechanisms, especially in PDAC murine models. Although several questions remain, the consensus is that enhancing Kras expression to a certain threshold level sustains the proliferation of pancreatic ductal cells. Pancreatic cancer develops when this proliferation becomes uncontrolled (Ardito, Gruner et al. 2012, Navas, Hernandez-Porras et al. 2012, Molina-Arcas, Hancock et al. 2013).

1.1.3 Hypercoagulability in pancreatic cancer

In approximately 700 BC, the Indian surgeon Sushruta was the first person to find and report an association between thrombosis and carcinoma (Khorana 2003). The French physician Armand Trousseau unveiled that this association was not coincidental, and venous thromboses occurred more frequently in patients with malignancies in his 1865 cohort study; thereafter, Trousseau studied the hypercoagulative state in cancer (Bariety 1967). The first study to elucidate the correlation between pancreatic malignancy and thrombosis disorder began in 1938, and in comparison with the 15-25% prevalence of thrombosis in other types of cancers, more than 60% of pancreatic cancer patients were documented to experience thrombotic diseases (Sproul 1938). Recent studies have revealed more detailed information about the relationship between thrombosis and pancreatic cancer. Patients with malignant lesions located in the body and tail of the pancreas are more susceptible to developing thrombosis, and tumor location is therefore recognized as an independent risk factor for thrombosis (Sahni, Baker et al. 2000, Carmeliet 2001). Another study identified metastatic pancreatic cancer as an essential independent risk factor for thrombosis, with a 3.3-fold higher prevalence than that observed with localized lesions (Ikeda, Egami et al. 2003).

Over the past 100 years, researchers have attempted to understand the mechanisms of hypercoagulability in malignancy, and numerous assumptions have been proposed (Figure 2). However, unfortunately, till now no definite conclusion has been reached.

Concerning pancreatic cancer, tissue factor (TF) is of prime importance in accounting for the hypercoagulative state. TF is a transmembrane protein expressed mainly in the subendothelial cells of the vessel wall and triggers the extrinsic pathway of the blood

coagulation cascade. Moreover, TF can also increase the expression of vascular endothelial growth factor (VEGF) and silence the angiogenesis inhibitor thrombospondin in the tumor extracellular matrix, promoting angiogenesis and thereby facilitating tumor spread (Yao, Ryan et al. 2009, Alkim, Sakiz et al. 2012, Wang, Sang et al. 2016). Some clinical studies have shown that a poor cancer prognosis is associated with high expression of TF in pancreatic cancer cells (Zhang, Deng et al. 1994, Kakkar, Lemoine et al. 1995, Shigemori, Wada et al. 1998, Ueno, Toi et al. 2000). To explain why thrombosis typically develops in extremities that are remote from the original tumor, scientists have hypothesized that TF-positive microvesicles (MV) could be involved. Specifically, TF-positive MVs are shed from cancer cells into the bloodstream and can thereby reach different organs. In this case, blood coagulation can be triggered at a remote site. This hypothesis has already been confirmed in a mouse model, but further studies in humans are required (Tesselaar, Romijn et al. 2007, Geddings and Mackman 2013).

Some studies show that pancreatic cancer cells can secrete some prothrombotic proteins and consequently enhance thrombosis. Heparanase, in addition to its procoagulant activity, plays a pro-metastatic role by degrading the extracellular matrix (Nadir and Brenner 2016). Heparanase reduces the activity of tissue factor pathway inhibitor (TFPI) and thereby enhances the activity of TF (Nadir 2020).

Pancreatic cancer cells can also release proteins that impede fibrinolysis, of which plasminogen activator inhibitor (PAI-1) is one of the most crucial. Both cytokines and activated platelets can locally activate PAI-1 and consequently inhibit fibrinolysis (Andren-Sandberg, Lecander et al. 1992).

Often, a higher level of activated platelets can be detected in pancreatic cancer patients' plasma compared to healthy blood donors, indicating that their hypercoagulability could be partly attributed to abnormal activation of platelets. This activation may also result from proteins secreted by pancreatic cancer cells, such as mucin and podoplanin (PDPN). PDPN appears to be a poor prognostic indicator in pancreatic cancer (Mezouar, Frere et al. 2016, Hirayama, Kono et al. 2018, Krishnan, Rayes et al. 2018).

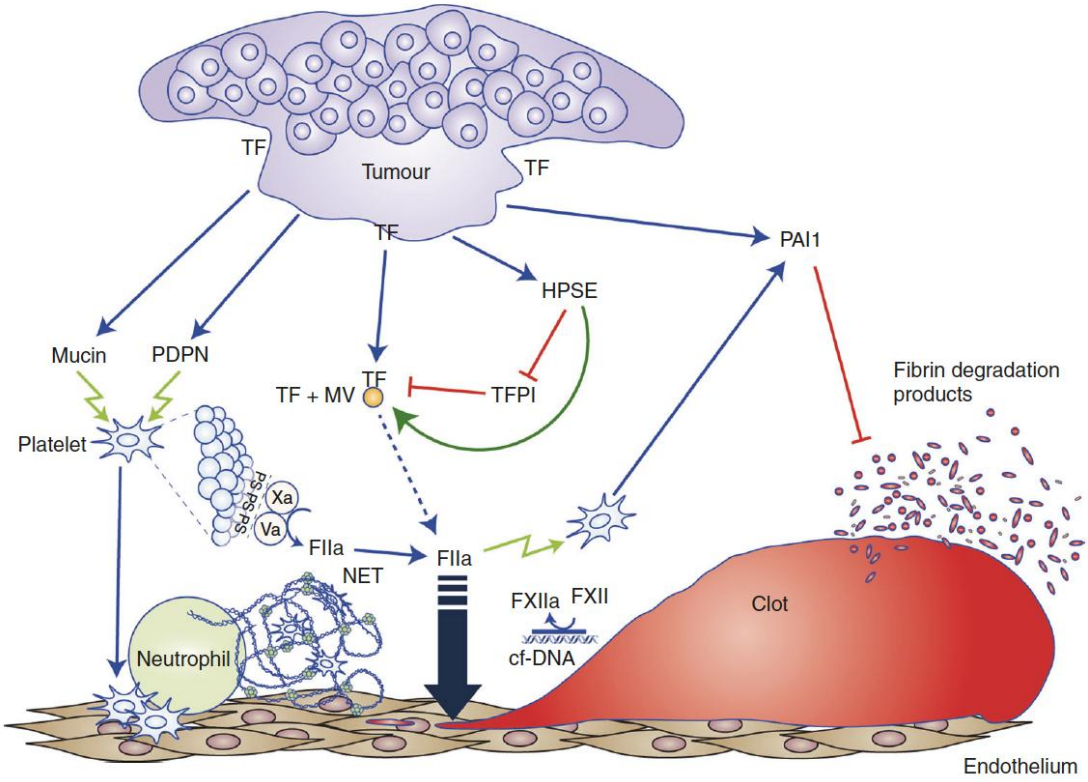

Figure 2 Major procoagulant effects in pancreatic cancer. See Ref (Campello, Ilich et al. 2019)

1.1.4 Metastasis

Metastasis indicates the spread of cancer cells from the primary tumor side to remote sites (Klein 2008). Metastasis involves different steps, including tumor cells' intravasation, circulation and extravasation at the site of metastasis formation. Cancer cells can migrate and intravasate into the vessel system, including not only the blood vessels but also the lymphatic vessels; thereafter, these cells become circulating cancer cells (Maheswaran and

Haber 2010). Very rarely, these cells evade the blood-based immune system. Indeed, the blood system is under strict surveillance by systemic immune cells; therefore, most circulating tumor cells are detected and eliminated, and only a small number escape immune surveillance. After administrating tumor cells through the tail vein, less than 0.1% of the injected tumor cells survive and, finally, form the premetastatic niche (Butler and Gullino 1975, Chang, di Tomaso et al. 2000, Wong, Lee et al. 2001).

1.2 Extracellular vesicles (EVs)

1.2.1 Overview of EVs

Analysis by electron microscopy and other nanoscopic imaging techniques allows scientists to study EVs. There are many different types of EVs (Figure 3).

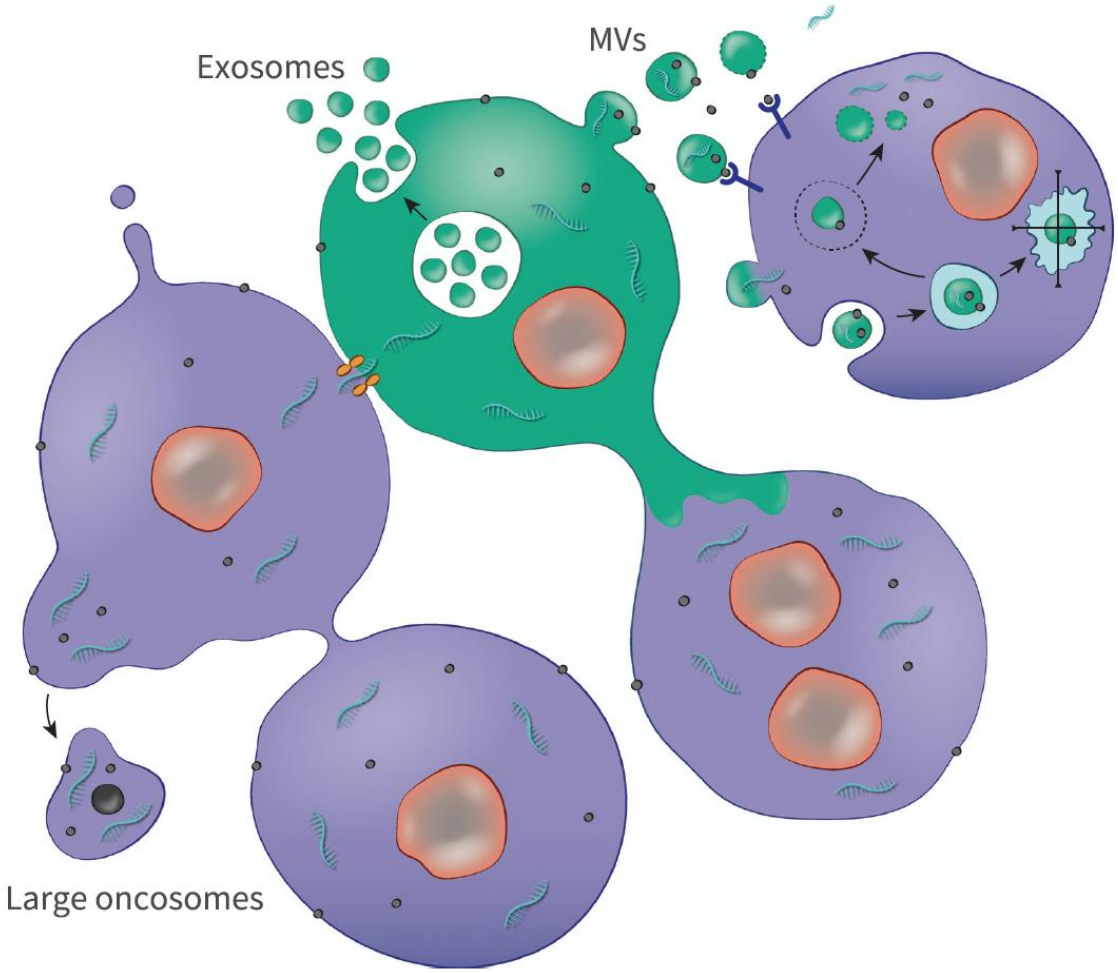

Figure 3 Different subtypes of EVs in cell-to-cell communication. See Ref (Maas, Breakefield et al. 2017)

Exosomes originate from multivesicular bodies (MVBs), while ectosomes or microvesicles are shed directly from the plasma membrane. Exosomes are usually smaller than 150 nm; hence, some researchers call them small EVs (sEVs). Ectosomes or microvesicles/microparticles are usually larger, with diameters ranging from 200-500 nm. Usually, the size of the vesicles indicates their origin. Moreover, other types of vesicles exist, such as large oncosomes, a group of gigantic vesicles budding outward from cancer cells (usually 1-10 μm in diameter), and apoptotic bodies, a subtype of vesicles released during apoptosis. Hence, currently, the nomenclature of EVs tends to be related to vesicle

biogenesis to reduce misunderstandings (Nabhan, Hu et al. 2012, Rilla, Siiskonen et al. 2014, Minciacchi, Freeman et al. 2015, Tkach and Thery 2016).

EVs were discovered in the late 1960s, and our knowledge of these small vesicles has since greatly increased (Wolf 1967). EVs were recognized as "cell debris"; however, their lipid and protein components were later revealed (Dalton 1975). In the past ten years, interest in EVs has strongly increased due to two crucial findings. First, EVs were found in various body fluids, such as blood, urine and breast milk. Thus, EVs can act as transmitters of signals to remote sites. Second, different subtypes of RNAs were detected inside these vesicles. Such RNA species are stabilized against hydrolysis by RNases in the surrounding vesicle membrane. Numerous studies have shown that EVs can transfer RNAs between different cells (Skog, Wurdinger et al. 2008, Cocucci, Racchetti et al. 2009, Abels and Breakefield 2016, Tkach and Thery 2016).

The molecular mechanisms underlying this communication are still not entirely clear. Through endocytosis, EVs can be internalized by acceptor cells, and thereafter, their content can be released into the cytoplasm. Alternatively, internalized EVs can be degraded in the lysosome, and some of the intravesicular components of EVs, such as proteins and nucleic acids, can then be translocated to the cytoplasm. Moreover, EVs can directly interact with cognate receptors in the cell membrane without being internalized, and signals can subsequently be transduced into the cells through different pathways. Unlike endocytosis-dependent mechanisms, this transmission mechanism is restricted to certain cell types, and the signal in the acceptor cell can be evoked rapidly. These two communication modes are observed in physiological conditions and tumor settings (Costa-Silva, Aiello et al. 2015, Hoshino, Costa-Silva et al. 2015, Eitan, Suire et al. 2016).

1.2.2 EVs in cancer

EVs have been widely detected in the body fluids of cancer patients and, as a result, increasing attention has been devoted to the role of EVs in cancer development. In addition to contributing to the formation of the premetastatic niche, EVs are involved in the establishment of the tumor microenvironment (TME) (Maas, Breakefield et al. 2017).

The TME is essential for both tumorigenesis and metastasis. For example, endothelial cells can be educated by tumor-released EVs, driving the establishment of new blood vessels (angiogenesis) with high permeability. These processes enable tumor cells to acquire nutritional support and to form premetastatic niches. Fibroblasts, considered one of the most pivotal factors impeding tumorigenesis, can be transformed by EVs to demonstrate a pro-tumorigenic phenotype. These pro-tumorigenic fibroblasts are referred to as cancer-associated fibroblasts (CAFs) (Fabbri, Paone et al. 2012, Gross, Chaudhary et al. 2012, Phinney, Di Giuseppe et al. 2015). Moreover, tumor-derived EVs educate immune cells. The antitumor functions of immune cells can be suppressed by the transmission of oncogenes to the cells via EVs (Greco, Hannus et al. 2001, Beckett, Monier et al. 2013).

Recognizing the importance of the formation of premetastatic niches represents a major advance in metastasis research, as it sheds light on why certain types of cancer cells prefer to metastasize to specific organs. Circulating tumor cells and metastatic organs can be considered seeds and soils (Fidler 2003). Currently, it is believed that some tumor-derived substances, especially EVs, act as indispensable fertilizers. After interaction with tumor-derived EVs, the perivascular microenvironment in the metastatic organ can be remodeled and reshaped (Kucharzewska, Christianson et al. 2013, Lopez-Verrilli, Picou et al. 2013, Jarmalaviciute and Pivoriunas 2016).

1.3 Immune cells relevant for vascular metastasis

1.3.1 Overview of monocytes

Monocytes are a subtype of leukocytes and were described over a hundred years ago as phagocytic mononuclear cells. In the 1970s, the mononuclear phagocyte system (MPS) concept was proposed, revealing that monocytes were critically responsible for different innate immune responses (Murray, Webb et al. 1926, van Furth and Cohn 1968, van Furth, Cohn et al. 1972). Monocytes are generated in the bone marrow (BM) and are similar to the other myeloid cells derived from common myeloid progenitors (CMPs). These CMPs can differentiate into granulocytic myeloid progenitors (GMPs) and then subsequently into macrophage dendritic cell progenitors (MDPs) and eventually transform into common monocyte progenitors (cMoPs). cMoPs are considered direct precursors of circulating monocytes. Circulating monocytes can migrate into infected or damaged tissues and differentiate into macrophages or myeloid lineage dendritic cells (Akashi, Traver et al. 2000, Fogg, Sibon et al. 2006, Hettinger, Richards et al. 2013).

In the last 50 years, a significant breakthroughs in our understanding of monocyte physiology was made, categorizing monocytes into 3 heterogeneous subgroups. These are "*classical monocytes or inflammatory monocytes ($CD14^+CD16^-$ in humans/$Ly6C^{high}CD11b^+$ $CX3CR1^{low}$ in mice), non-classical monocytes or patrolling monocytes ($CD14^{low}$ $CD16^+$ in humans/$Ly6C^{low}$ $CX3CR1^{high}$ in mice) and intermediate monocytes ($CD14^+CD16^+$ in humans)*" (Sprangers, de Vries et al. 2016). Intermediate monocytes may be monocytes transitioning from classical monocytes to non-classical monocytes (Figure 4).

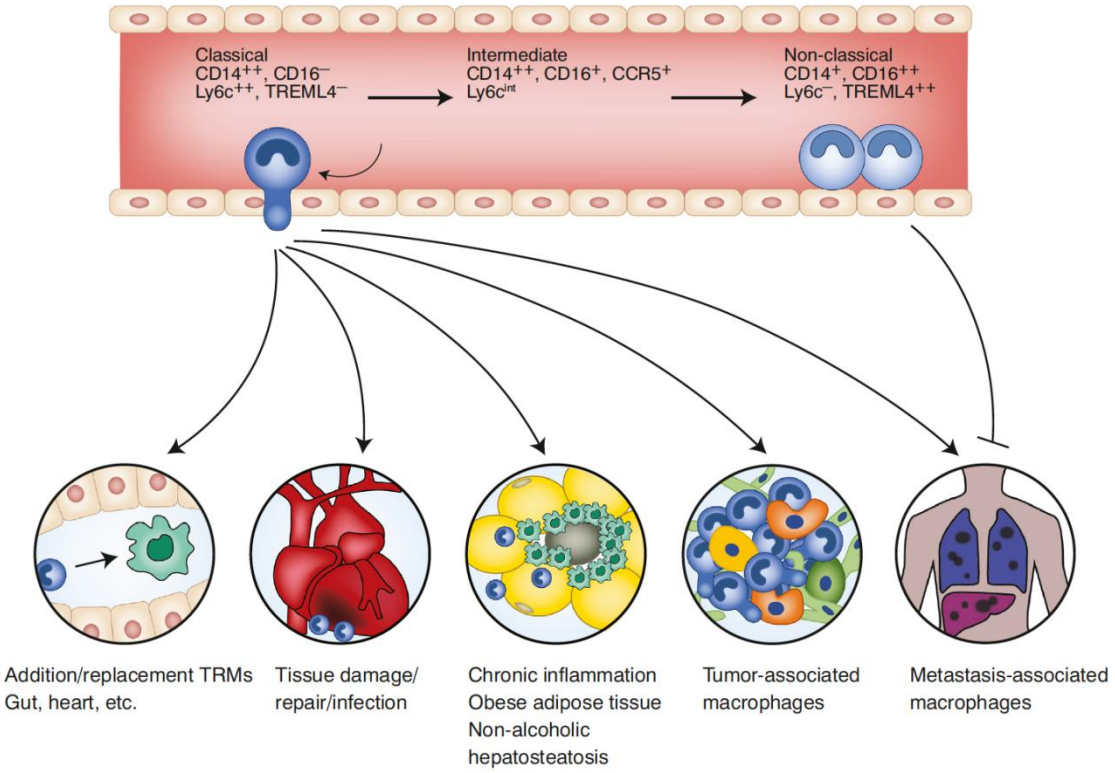

Figure 4 Differentiation of human and mouse monocytes in peripheral blood. See Ref (Robinson, Han et al. 2021)

Therefore, it is likely not plausible to regard intermediate monocytes as a definite subtype of monocytes (Geissmann, Jung et al. 2003, Ziegler-Heitbrock, Ancuta et al. 2010). Mediated by the C-C chemokine receptor 2 (CCR2), classical monocytes can exit the BM and circulate in the peripheral blood. However, the lifespan of mature classical monocytes in humans and mice is only 1 day, and after that, they can either convert into macrophages or non-classical monocytes (Serbina and Pamer 2006, Jakubzick, Gautier et al. 2013, Yona, Kim et al. 2013, Patel, Zhang et al. 2017). Under physiological conditions, only 1% of classical monocytes differentiate into non-classical monocytes, and it has been demonstrated that this differentiation is highly dependent on orphan nuclear receptor Nr4a1 using Nr4a1$^{-/-}$ mice (Hanna, Carlin et al. 2011). Non-classical monocytes are involved in patrolling the endothelial cells in different vascular beds. Unlike classical monocytes, non-classical monocytes have a longer lifespan; 7 days in humans and 2 days in mice. This

relatively long lifespan ensures that a considerably large pool of non-classical monocytes is available that can eventually be replenished by the conversion of classical monocytes (Debien, Mayol et al. 2013, Lavin, Kobayashi et al. 2017).

1.3.2 Monocytes in Cancer

Monocytes can be recruited to tumor cells at all phases of tumorigenesis (Cho, Seo et al. 2018, Devalaraja, To et al. 2020). Monocytes can induce cancer cell death in different ways. Moreover, monocytes can engulf tumor materials, such as cell debris or EVs, through phagocytosis (Gordon and Freedman 2006, Headley, Bins et al. 2016, Yeap, Wong et al. 2017). Tumor EVs can inhibit this engulfment through the expression of CD47. CD172a is a receptor for CD47 that is widely expressed on the surface of monocytes. Poorer cancer prognosis is consistent with high expression of CD47 in different cancer types (Jaiswal, Jamieson et al. 2009, Chao, Alizadeh et al. 2010, Willingham, Volkmer et al. 2012). Although non-classical monocytes can theoretically increase the recruitment of NK cells, this largely depends on the number of non-classical monocytes that engulf tumor material. Since the number of non-classical monocytes represents less than 10% of total monocytes, the effect of monocytes on NK-cell recruitment is limited (Hanna, Cekic et al. 2015, Kubo, Mensurado et al. 2017, Plebanek, Angeloni et al. 2017). Monocytes that are differentiated into tumor-associated macrophages (TAMs) or monocyte-derived DCs (moDCs) are, in general, pro-tumorigenic (Anfray, Ummarino et al. 2019, Lurje, Hammerich et al. 2020). TAMs and moDCs can facilitate tumor cell extravasation and metastasis (Du, Lu et al. 2008, Lu, Weaver et al. 2012, Franklin, Liao et al. 2014).

1.4 The role of angiopoietins in tumor angiogenesis

Angiopoietins belong to the vascular growth factor family and are mainly responsible for angiogenesis during embryonic and postnatal development. Their receptor is the endothelial Tie-2 receptor. Angiogenesis encompasses several different processes, such as the sprouting of vessel buds, migration and proliferation of endothelial cells, and stabilization of both endothelial cells and mesenchymal cells. Angiogenesis plays a major role in the development of various diseases, ranging from autoimmune diseases to malignancies (Alves, Montalvao et al. 2010).

Four types of angiopoietins have been discovered: angiopoietin-1 (Ang-1), angiopoietin-2 (Ang-2), angiopoietin-3 (Ang-3), and angiopoietin-4 (Ang-4). Several angiopoietin-like proteins have also been identified. Angiopoietins consist of *"an N-terminal super clustering domain (SCD), a central coiled-coil domain (CCD) for ligand homo-oligomerization, a linker region, and a C-terminal fibrinogen-related domain (FReD) for binding to the Tie-2 receptor"(Zhang 2020)*. Ang-1 and Ang-2 can form dimers, trimers, and tetramers. Formation of such oligomers is a crucial step for their function, as Tie-2 can be activated only by Ang-1 oligomers, and only oligomerized Ang-2 can antagonize Ang-1 (Davis, Papadopoulos et al. 2003, Kim, Choi et al. 2005). Perivascular cells such as pericytes, vascular smooth muscle cells, fibroblasts, and tumor cells are the major cells expressing Ang-1(Jones, Master et al. 1999, Jones, Chen et al. 2003). Ang-2, an antagonist of Ang-1, is a secreted protein, which is strongly expressed in endothelial cells. Ang-2 is stored in Weibel-Palade bodies and can be released through autocrine mechanisms. Ang-2 destabilizes endothelial cells and increases their permeability. Thus, Ang-1 and Ang-2 jointly maintain vascular homeostasis (Oh, Takagi et al. 1999, Kim, Kim et al. 2000, Yuan, Khankin et al. 2009).

2. Objectives of the thesis

PDAC is the most procoagulant malignancy in the digestive system; thus, anticoagulant therapy is recommended for these patients (Sproul 1938, Campello, Ilich et al. 2019). Previous work suggests that tumor-driven fibrin formation at the site of metastasis might recruit non-classical monocytes and that the recruited monocytes could play a pivotal role in regulating tumor cell extravasation. However, the underlying mechanisms of these effects are unclear. In the present study, the following questions were addressed:

1. Does tumor-associated fibrin formation in the liver microcirculation recruit non-classical monocytes in response to pancreatic cancer cells? What is the underlying mechanism enabling fibrin to affect non-classical monocytes?
2. How could monocytes regulate the extravasation of pancreatic tumor cells?
3. What is the effect of EVs on tumor cell extravasation, and why are non-classical monocytes pro-metastatic after interacting with tumor-derived EVs?

3. Materials and methods

3.1 Materials

3.1.1 Equipment

Table 1 Equipment

Items	Company, Type
Analytical balance	VWR, Avantor
Acidimeter (pH value)	HI211, HANNA
CO_2 Incubator	CB-S170, Binder
Centrifuge Mikro 22R	Hettichlab
Centrifuge Universal 32	Hettichlab
Centrifuge Rotina 35	Hettichlab
Cell culture: Lamin Air flow MSC1.2	Thermo Scientific
Cell sorter	Beckman Coulter
Cryotome decive	Leica CM3050
Electrophoresis and membrane-transferring unit	BIO-RAD Mini-PROTEAN® Tetra System
Film development device	CURIX60, AGFA
LSM 510 Meta (confocal microscope)	Carl Zeiss
LSRFortessa™ Flow Cytometer	BD bioscience
Micropipettes 2.5 µl	Eppendorf
Micropipettes 10 µl	Eppendorf
Micropipettes 20 µl	Eppendorf
Micropipettes 100 µl	Eppendorf

Micropipettes 200 µl	Eppendorf
Micropipettes 1000 µl	Eppendorf
Neubauer chamber	Improved, Brand
Optical microscope	Axiovert 100, Carl Zeiss
Pipet boy	Ratiolab
Power supply unit (WB)	BIO-RAD, PowerPAC™ HC
Sarstedt serological pipette 5ml	Sarstedt
Sarstedt serological pipette 10ml	Sarstedt
Sarstedt serological pipette 25ml	Sarstedt
Sarstedt serological pipette 50ml	Sarstedt
SpectraMax Plate reader	Molecular Devices
Thermomixer R	Eppendorf
Thermostat water bath	Julabo Labortechnik
Ultracentrifuge	Beckman, Optima™, LE-80K
Vortex Genie 2	Bender & Hobein AG

3.1.2 Kits

Table 2 Kits

Item	Company	Catalog number
Alexa488™ Protein Labeling Kit	Invitrogen™	A20181
Alexa555™ Protein Labeling Kit	Invitrogen™	A20187
Alexa555™ Protein Labeling Kit	Invitrogen™	4387406
Alexa594™ Protein Labeling Kit	Invitrogen™	A10239

3.1.3 Primary antibodies

Table 3 Primary antibodies

Antibody	Reactivity	Concentration	Host	Company	Catalog number
α-CD4	Mus	1:100	Rattus	BioLegend®	100442
α-CD8a	Mus	1:100	Rattus	BioLegend®	100702
α-CD45	Mus	1:50	Rattus	AbD Serotec	MCA1031GA
CD11b (M1/70)	Mus	50μg / Mus	Rattus	Biolegend	101202
α-Ang-1	Mus	1:200-1:500	Rabbit	Abcam	ab8451
α-Ang-2	Mus	1:200-1:500	Rabbit	Abcam	ab8452
α-mNKp46	Mus	1:500	Goat	BioLegend®	AF2225
α-CX3CR1	Mus	1:50-1:200	Rabbit	Novus Biologicals	bs-1728R
α-F4/80	Mus	1:100-1:200	Rattus	BioLegend®	123102
α-Fibrin	Human	1:150-1:300	Mus	WAK	NYBT2G1
α-Ly6C	Mus	1:200-1:400	Rattus	Invitrogen™	1804
α-Ly6G	Mus	1:50-1:200	Rattus	BD Biosciences	551459
Mouse IgG	Mus	-	Mus	Vector BioLab	BA9200
Rabbit IgG	Mus	-	Rabbit	Vector BioLab	I-1000
Rat IgG	Mus	-	Rattus	Vector BioLab	I-4000
α-Stabilin II	Mus	1:200	Rattus	MBL	D317-4

3.1.4 Secondary antibodies

Table 4 Secondary antibodies

Antibody	Reactivity	Concentration	Host	Company	Catalog
Alexa Fluro 488®	Mus	1:500-1:2000	Donkey	Invitrogen™	A32766
Alexa Fluro 488®	Rattus	1:500-1:2000	Goat	Invitrogen™	A48262
Alexa Fluro 488®	Rabbit	1:500-1:2000	Goat	Invitrogen™	A110341
Alexa Fluro 488®	Goat	1:500-1:2000	Donkey	Invitrogen™	A110551
Alexa Fluro 546®	Mus	1:500-1:2000	Goat	Invitrogen™	A110301
Alexa Fluro 546®	Rattus	1:500-1:2000	Goat	Invitrogen™	A110811
Alexa Fluro 546®	Rabbit	1:500-1:2000	Goat	Invitrogen™	A110351
Alexa Fluro 594®	Mus	1:500-1:2000	Goat	Invitrogen™	A327421
Alexa Fluro 594®	Rattus	1:500-1:2000	Goat	Invitrogen™	A110071
Alexa Fluro 594®	Rabbit	1:500-1:2000	Goat	Invitrogen™	A110371
IgG-HRP	Rabbit	1:500-1:2000	Chicken	Santa Cruz	Sc-2955

3.1.5 Antibodies for FACS and cell sorting

Table 5 Antibodies for FACS and cell sorting

Antibody	Reactivity	Dilution	Host	Label	Company	Catalog number
α-Ly6G	Mus	1:150	Rat	FITC	BioLegend	127605
α-Gr-1	Mus	1:200	Rat	APC	BioLegend	108411
α-Gr-1	Mus	1:100	Rat	Percp/Cy5.5	BioLegend	108427
α-CD45	Mus	1:200	Rat	APC/Cy7	BioLegend	368515
α-CD11b	Mus	1:150	Rat	FITC	BioLegend	101205
α-CD115	Mus	1:150	Rat	BV421	BioLegend	135513
α-CD3	Mus	1:150	Rat	FITG	BioLegend	100203
α-CD4	Mus	1:150	Rat	APC	BioLegend	100411
α-CD8a	Mus	1:150	Rat	BV421	BioLegend	100737
α-CD49b	Mus	1:100	Rat	APC	BioLegend	103515
α-F4/80	Mus	1:100	Rat	FITC	BioLegend	123107

3.1.6 Buffers

Blocking buffer (for staining)

Sterile phosphate buffered saline

2% BSA

0.1%-0.5% Tween 20

Ca^{2+}/Hepes buffer (activation of fibrin formation)

10 mM Hepes

100 mM $CaCl_2$,

ddH_2O, pH 7.4

Phosphate Buffered Saline (PBS for washing in process of staining) (1L)

8 g NaCl

0.2 g KH_2PO_4

0.2 g KCl

1.42 g $Na_2HPO_4 \cdot 2H_2O$

Tris Buffered Saline (10 X)

0.2M Tris base

1.5M NaCl

ddH_2O, pH 7.2-7.4

Permabilisation buffer

Sterile phosphate buffered saline

0.5 % - 2% BSA

0.1 % Triton-100x

Tryphan Blue in Phosphate Buffered Saline (calculation of cells)

Sterile commercial Phosphate Buffered Saline 1X

1 mM $CaCl_2$

0.4% Tryphan blue

SDS-PAGE transfer buffer (250ml)

NUPAGE Transfer buffer 1X (dilution in ddH_2O)

0.1% Antioxidant

20% Methanol

Blocking buffer for WB membrane (1L)

1% Tween 20

5% skimmed dry milk (BSA)

Tris buffered saline

Filter with 0.2 mm Whatmann filter paper

Washing buffer for WB membrane (1L)

0.3% Tween 20

Tris buffered saline

FACS Buffer (500ml)

500ml 1X PBS

2% BSA

2nM EDTA

3.1.7 Cell lines

Table 6 Cell lines

Cell ID	Sample	Survival (days)	Metastasis (Yes/No)	Resources & Morphology	Genomic Kras status
Cell 5320	PDAC	466	Yes	Mus Mesenchymal	$Kras^{G12D}$, CN-LOH
Cell 16990	PDAC	377	No	Mus Epithelial	$Kras^{G12D}$, het
Cell S134	PDAC	274	Yes	Mus Mesenchymal	$Kras^{G12D}$, amp-focal
Cell 53631	PDAC	478	Yes	Mus Epithelial	$Kras^{G12D}$, amp-arm
Cell 8028	PDAC	275	Yes	Mus Mesenchymal	$Kras^{G12D}$, CN-LOH
Cell 8182	PDAC	508	No	Mus Epithelial	$Kras^{G12D}$, het
Cell 8305	PDAC	305	Yes	Mus Epithelial	$Kras^{G12D}$, amp-arm
Cell 8570	PDAC	263	Yes	Mus Mesenchymal	$Kras^{G12D}$, CN-LOH
Cell 8661	PDAC	470	Yes	Mus Epithelial	$Kras^{G12D}$, amp-arm
Cell 9091	PDAC	390	Yes	Mus Mesenchymal	$Kras^{G12D}$, CN-LOH
Cell 9203	PDAC	NA	Yes	Mus Epithelial	$Kras^{G12D}$, het

3.1.8 Mouse models

Table 7 Mouse models

Mouse model	Resources
Wild type mouse model: C57BL/6 M/F 21-25 G ca. 8+ weeks	Charles River
Nr4a1se_2$^{-/-}$ mouse model: C57BL/6-Rr39^{em1Ched}/J, M/F 21-25 G ca. 8+ weeks	The Jackson Laboratory (Stock No: 030204), Institute für Prophylaxe und Epidemiologie der Kreislaufkrankheiten, Ludwig-Maximilian-Universität München

3.1.9 Reagents and chemicals

Table 8 Reagents and chemicals

Item	Company	Catalog number
Aceton Kunst >99.8%	Carl Roth GmbH+ Co.	9372.6
Acrylamide/Bis-Acrylamide, 30% Lösung	Sigma-Aldrich	A3574
Acetic acid 1L 100%	Carl Roth GmbH+ Co.	6755.1
Antioxidant	NuPAGE™	NP0005
Falcon® Cell culture bottle (175cm^2)	Falcon®, Corning	353028
Falcon® Cell culture bottle (75cm^2)	Falcon®, Corning	353024
DAKO Pen	Dako Denmark A/S	S2002
Dulbecco's Modified Eagle Medium High Glucose	Gibco®	41965039
Ethanol (99.8%)	Sigma-Aldrich	V001229
Fetal Bovine Serum	Gibco®	A31605
Ibidi Freezing Medium Classic	Ibidi	80022
Hydrochloric acid 37%, fuming	Carl Roth GmbH+ Co.	4625.1
KOH	Carl Roth GmbH+ Co.	K017.1
Methanol ROTISOLV® HPLC	Carl Roth GmbH+ Co.	KK39.2
Cellstar® 6 well cell culture plate	Cellstar®	657160
Cellstar® 12 well cell culture plate	Cellstar®	665102
Cellstar® 24 well cell culture plate	Cellstar®	662160
Cellstar® 96 well cell culture plate	Cellstar®	655160

Sodium chloride >99,8%	Carl Roth GmbH+ Co.	9265.2
Sodium hydroxide 1L	Carl Roth GmbH+ Co.	K021.1
SuperFrost Plus™ Adhäsionsobjektträger	Fisher scientific	10149870
Phosphate buffered saline	Sigma-Aldrich	RNBJ9564
Poly-L-Lysine 0.1% (w/v) in H_2O	Sigma-Aldrich	P8920
Mini Protease Inhibitor Cocktail	EMERALD	11836153001
Protein Assay Reagent A	BIO-RAD	5000113
Protein Assay Reagent B	BIO-RAD	5000114
Eppendorf Safe-Lock Tube (1.5ml)	Eppendorf Quality™	0030120159
Eppendorf Safe-Lock Tube (2ml)	Eppendorf Quality™	0030120205
O.C.T.™ Compound Containing	SAKURA®	2012102832
Trypan Blue 0.4% for microscopy	Carl Roth GmbH+ Co.	1680.1
Trypsin-Lösung aus Schweinepankreas	Sigma-Aldrich	59418C-100ML
Tween® 20, for molecular biology, viscous liquid	Sigma-Aldrich	P9416
40 µm Cell strainer	Falcon®, Corning	352340
100 µm Cell strainer	Falcon®, Corning	352360
15ml centrifuge tube	Falcon®, Corning	352096
50ml centrifuge tube	Falcon®, Corning	352070
4% to 12% Bis-Tris, 1.5mm, Mini Protein Gel, 10 well	NuPAGE™	NP0335BOX
RIPA-Lyse und Extraktionspuffer	Thermo Scientific™	89901
Protease Inhibitor	Thermofisher	36978

MOPS SDS Running Buffer	NuPAGE™	NP0001
Transfer Buffer	NuPAGE™	NP00061
Tris buffered saline (TBS-T)	SuperBlock™	37535
ECL Western Blotting Substrate	Pierce™	32106
ECL Prime Western Blotting System	Sigma-Aldrich	GERPN2232

3.2 Methods

3.2.1. Animal experimentation protocol

C57BL/6 mice and Nr4a1se_2$^{-/-}$ (C57BL/6-Rr39^{em1Ched}/J) mice were purchased from Charles River Laboratory and Jackson Laboratory. The mice were maintained in the pathogen-free animal facility in Walter Brendel Centrum (WeBex). All experiments were performed in mice aged 9 weeks to 14 weeks. All the animal experiments were approved by the local Animal Experimentation Committee (Regierung of Oberbayern, Munich) and were performed in accordance with the ARRIVE guidelines and regulations. At the end of the experiment, under inhalation anesthesia with isoflurane, mice were sacrificed by strangulating their neck and then the liver was harvested for further analysis.

3.2.2. Injection protocols

Briefly, 2×10^6 of CMPTX-stained PDAC cells were dissolved in a total of 350 µl phosphate-buffered saline and administrated through the tail vein. Apart from WT mice, also rivaroxaban-treated animals as well as Nr4a1se_2$^{-/-}$ mice were analyzed as indicated in Figure 5.

Rivaroxaban is a selective FXa inhibitor widely prescribed to patients with thrombotic disorders. 2-4h after administration of rivaroxaban, the blood concentration could reach its peak value and the half-time of its plasma elimination occurs after 9 h (Mueck, Stampfuss et al. 2014). Therefore, rivaroxaban (3mg/kg) is administrated through tail vein into mice 4h before tumor cell injection. 6h after tumor cells injection, mice were sacrificed, and the liver was collected for further analysis.

Due to the pivotal effect of Nr4a1 on differentiation from Ly6C^{high} to Ly6C^{low} monocytes, Nr4a1se_2$^{-/-}$ mice model was predominant in non-classical monocytes' studies. Differentiation from classical monocytes to non-classical monocytes was blocked in Nr4a1$^{-/-}$ mice. However, meanwhile, the transformation from monocytes to tissue macrophage was largely inhibited in traditional Nr4a1$^{-/-}$ model as well. In this study, Nr4a1se_2$^{-/-}$ model was applied. In this model, a Nr4a1 super-enhancer was deleted in the upstream of Nr4a1 gene fragment and this depletion was proved not to reduce the transformation from monocytes to macrophage (Thomas, Hanna et al. 2016).

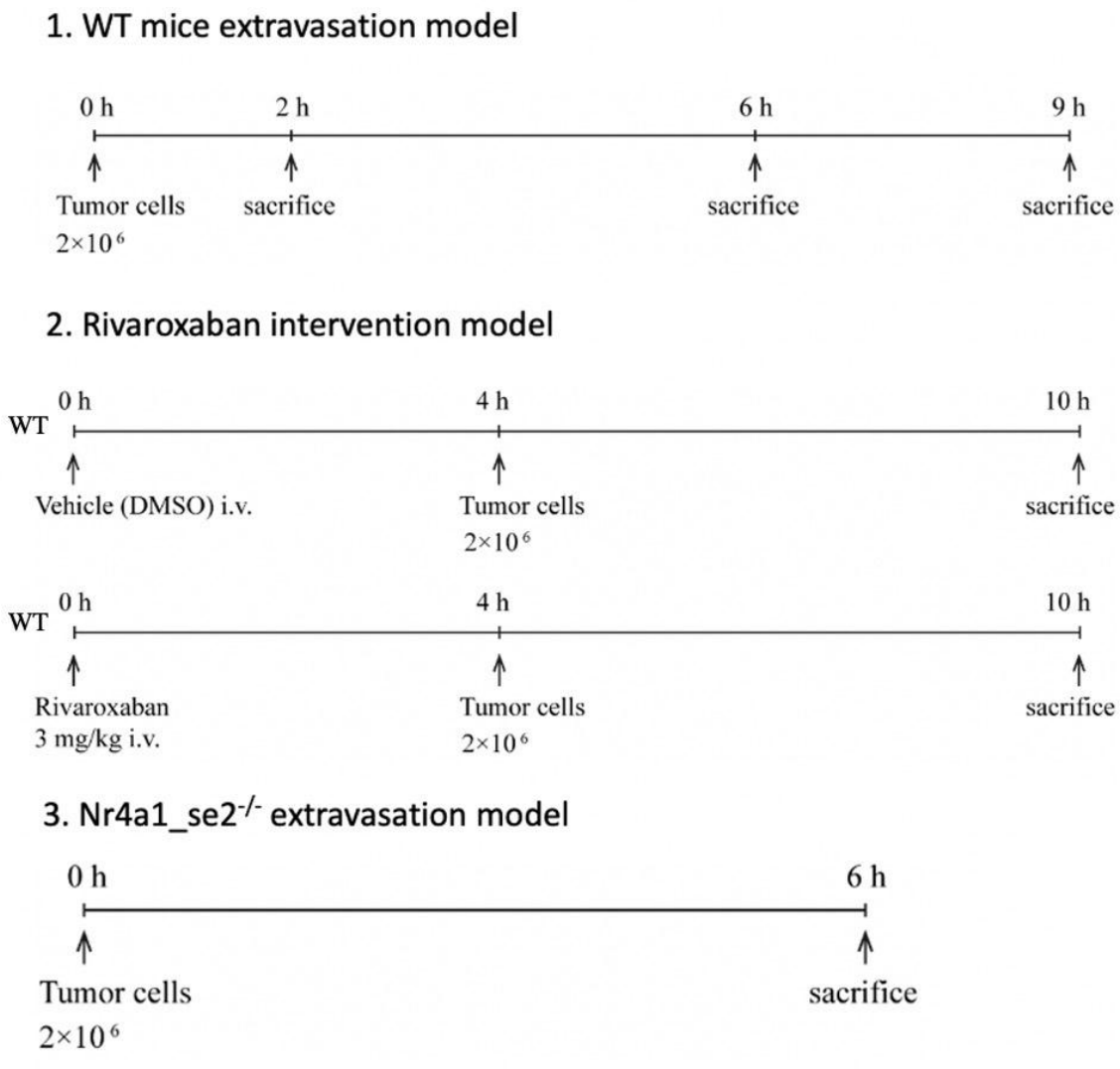

Figure 5 Detailed protocols of animal models

3.2.3 Organ preparation at the end of animal experiments

Under inhalation anesthesia with isoflurane mice were sacrificed by strangulating their neck. In order to prevent the tissue degradation, organs were removed rapidly through a cross incision across the chest and abdomen in the mice. After the collection of organs, they were rinsed with phosphate-buffered saline for several times to remove the contamination of blood. Then the organs were fixed in 4% PFA solution for 1-2 h and dehydrated in sucrose solution with gradient concentrations from 10% to 30% overnight. The storage temperature was set as -80 ˚C.

3.2.4 Tissue cryosections

Tissues harvested from mice were stored at -80˚C before use and were embedded into Tissue-Tek O.C.T.^{TM} prior to cryosection. Tissues were cut into sections with a width ranging from 10-20 μm and were stored at -20˚C. Each section has to be check under light microscope to ensure its intactness.

3.2.5 Tumor cell culture

All the tumor cells referred before (see Table 6) were cultured in DMEM medium with 4.5% glucose with 10% FBS, 100 units/ml penicillin, and 0.1 mg/ml streptomycin. The cells were grown in cell culture flasks in a cell incubator (incubation conditions: 37 ℃ with 20% O_2 and 5% CO_2). 1xTrypsin-EDTA solution was employed to split the cells when they were confluent. Cells were stored as cell stocks in -80 ˚C with Cryoprotectant Medium.

3.2.6 Cell lysis

We used RIPA lysis buffer (See Reagents) and plastic cell scrapers to lyse the cancer cells. After 20 min centrifugation at 16,000g, cell debris was removed by discarding the supernatant. The pellet containing the cell lysate was analyzed for protein concentration.

3.2.7 Protein estimation

We utilized the Bradford assay to estimate the concentration of cellular proteins. Standard serum bovine albumin was diluted into different concentrations in accordance with the instructions from reagent manufacturer using phosphate-buffered saline as medium (from 2 mg/ml to 0.03906 mg/ml). 5 µl respective samples and 25 µl solution A were pipetted onto 96-well plate in triplicates. Then 200 µl of solution B was added, and, after 15 min, a plate reader was applied to detect the absorbance at 750 nm. With the help of a standard curve, the concentration of samples could be calculated.

3.2.8 SDS-PAGE and Western blot

Depending on the different molecular weights of the target protein, we selected polyacrylamide protein gels with a concentration from 7.5% to 15%. Protein lysates were denatured at 70 ℃ for 10 min with pre-added loading buffer. We added protein lysate into proper SDS-acrylamide gels. To control the molecular weight of the loaded protein lysate, a pre-stained protein ladder was applied.

In running buffer, the proteins were segregated by electrophoresis (running voltage: 80-120 V). Then, at a constant power supply (125 mA), we transferred all the separated proteins onto PVDF membranes by application of the Invitrogen blotting system with NuPAGETM Transfer buffer.

After blocking for 1h with either 5% skimmed milk or BSA in Tris-buffered saline, we incubated the blocked membranes in TBS with a respective concentration of primary antibodies (1:1000-1:5000) at 4℃ for at least 12 h. The detailed information for primary antibodies is indicated in Table 9. Next, the horseradish-peroxidase (HRP)-conjugated secondary antibodies were added and co-incubated with the membrane for 1 h at room temperature. The development machine was used to detect the ECL signals representing the respective proteins.

Table 9 Primary antibodies for Western Blotting

Antibody	Reactivity	Dilution	Host	Company	Catalog number
α-Ang-1	Mus/Human	1:1000	Rabbit	abcam	ab8451
α-Ang-2	Mus/Human	1:1000	Rabbit	abcam	ab8452
α-GAPDH	Mus/Human	1:3000	Rabbit	abcam	ab181602

3.2.9 Isolation of EVs

After tumor cells had reached confluent in culture flasks, they were cultured in vesicle-free medium for another 3 days. The supernatants were collected and centrifuged at 350 g for 5 min in order to remove the contamination of dead cells and of cell debris. The two subgroups of EVs were obtained after 20 min at 2000xg (large EVs or large oncosomes) and for 2h at 100,000xg without break (exosomes and microvesicles), respectively. EVs were present in the respective pellets and were maintained at -20 ℃.

3.2.10 Immunostaining of cryosections

Cryosections (10-15 μm) were thawed at room temperature for 10 min and fixed in 4% of formalin for 15 min. They were blocked with a blocking buffer for 40-60 min to reduce the non-specific staining. Primary antibodies were diluted with dilution buffer at the respective concentrations and incubated with cryosections overnight at 4˚C. Then after rinsing twice, they

were incubated with diluted secondary antibody for 1 h at room temperature. At the end, the mounting medium was put on the tissue sections and the slides were visualized using a confocal microscope (LSM 700 Carl-Zeiss Platform).

3.2.11 Imaging and Image analysis

Confocal laser scanning microscopy was applied to detect fluorescence signals in tissue sections or cells in culture. Using the Carl-Zeiss 510-CLSM system, the following emission signals could be detected: green (488nm), orange (555nm), and red (594nm) and were quantitively recorded by the detector. All the images were analysed with ZEN software (Blue 2009/ 2011; Black 2012).

3.2.12 Preparation of blood sample for flow cytometry (FACS) analysis and cell sorting

After inhalation anesthesia with isoflurane, MMF (90 µl 10% fentanyl+90 µl 30% medetomidine+15 µl midazolam) was injected into mice abdomen to enhance the sedative function of the isoflurane. 10-15 min after intensive anesthesia, pain reflexes of mice were checked. Only when pain reflexes disappeared, blood-drawing directly from left ventricle of the heart was allowed. Blood samples were then stored with anticoagulant on ice and lysed with 10X RBC lysis buffer 2-3 times. PBS was applied to terminate the lysis reaction after each time. Leukocytes were obtained after a 5min centrifugation step at 350xg.

3.2.13 Preparation of liver samples for flow cytometry (FACS) analysis

After drawing blood from the left ventricle of the heart, a small incision was made in the right atrium and 20ml PBS were injected slowly through left ventricle to perfuse the mice. Mice were sacrificed immediately after perfusion and livers were harvested in ice-cold PBS. Hepatic tissues were digested in a pre-warmed (37 ℃) digestive enzyme mixture (100 µl

collagenase+100µl dispase+100µl DNase I) for 20 min in an incubator and were meshed and filtered through a 40nm filter. We centrifuged the suspensions for 3 min at 50xg in order to remove hepatic cells and then collect the immune cells after a 5min centrifugation step at 350xg.

3.2.14 Isolation of non-classical monocytes isolation with cell sorter

Although the process of cell sorting with the cell sorter is time-consuming and requires the labelling of the target cells before isolation, it can sort almost all kind of cells and the sorted cells are in general of high purity than with other methods. We obtained immune cells from the spleen and the peripheral blood and identified non-classical monocytes as CD115+ and Gr-1- cells. The gating strategy for the sorting of non-classical monocytes is shown in Figure 6.

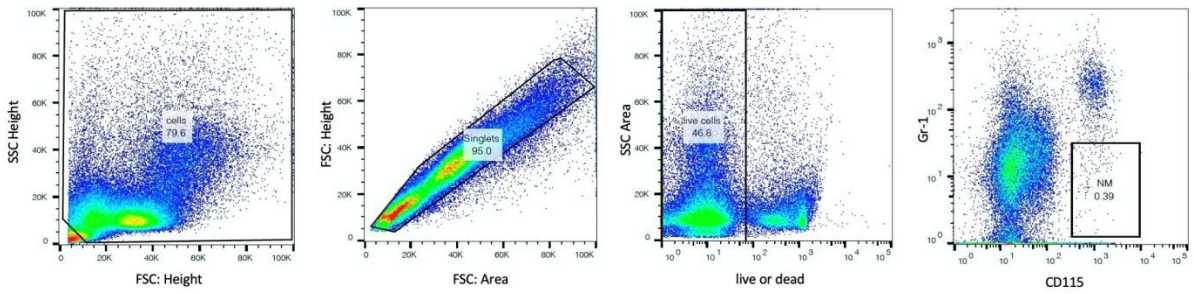

Figure 6 Gating strategy for sorting of non-classical monocytes

3.2.15 Flow cytometry (FACS) and cell sorting

The cells were stained in FACS buffer for 40-60 min. Multiparameter flow cytometric analysis was performed with a LSRFortessa^{TM} Flow Cytometer. The gating strategies were as follows: neutrophils (CD45+, Ly6G+), classical monocytes (CD45+, CD11b+, CD115+, Gr-1+), non-classical monocytes (CD45+, CD11b+, CD115+, Gr-1-), CD4+ T cells (CD3+, CD4+, CD8a-), CD8+ T cells (CD3+, CD8a+, CD4-), NK cells (CD49b+).

3.2.16 Statistical analysis

For comparison between data of multiple groups, one-way ANOVA with a post hoc Bonferroni correction was used. Two-tailed unpaired T-test was performed for the comparisons between two groups. The significance level of P values was set as < 0.05. The asterisks indicate the following P values: $*P < 0.05$, $**P < 0.01$, $***P < 0.001$ and $****P<0.0005$. Experiments were repeated at least 3 times and results are given as mean values $\pm$ SEM.

4. Results

4.1 Role of intravascular coagulation in the recruitment of non-classical monocytes

4.1.1 Determination of fibrin formation in microvessels *in vivo*

Previously, procoagulant screening via thromboelastography was performed in 11 PDAC cell lines sharing the $Kras^{G12D}$ mutation (Mueller, Engleitner et al. 2018). Cell lines 8182 and 53631 exhibited the strongest procoagulant activities, whereas cell line 9091 had the weakest procoagulant activity. To test the role of these cell lines *in vivo*, we injected them into the tail vein of C57BL/6 (WT) mice to compare their coagulation competence in the liver microcirculation. The mice were sacrificed 6 h after tumor cell injection, and the livers were removed to analyze fibrin formation in the liver microvessels. The fibrin depositions in the microcirculation were much lower in mice injected with cell line 9091 than in those that received cell line 8182 or cell line 53631 (Figure 7 a-c, f). Thus, the coagulation activities of the cell lines *in vivo* mimicked their activities *in vitro*. Rivaroxaban, a specific FXa inhibitor used clinically as an anticoagulant, was administered to inhibit fibrin formation in mice injected with 8182 and 53631 cells. WT mice were preinjected with rivaroxaban or its vehicle (DMSO), and after 4 h, cell lines 8182 and 53631 were injected through the tail vein. Six hours later, fibrin formation in liver microvessels was significantly decreased in rivaroxaban-treated mice compared with the DMSO group. Indeed, tumor-induced fibrin formation in the liver was reduced by almost 80% in mice treated with rivaroxaban (Figure 7 d, e, g, h).

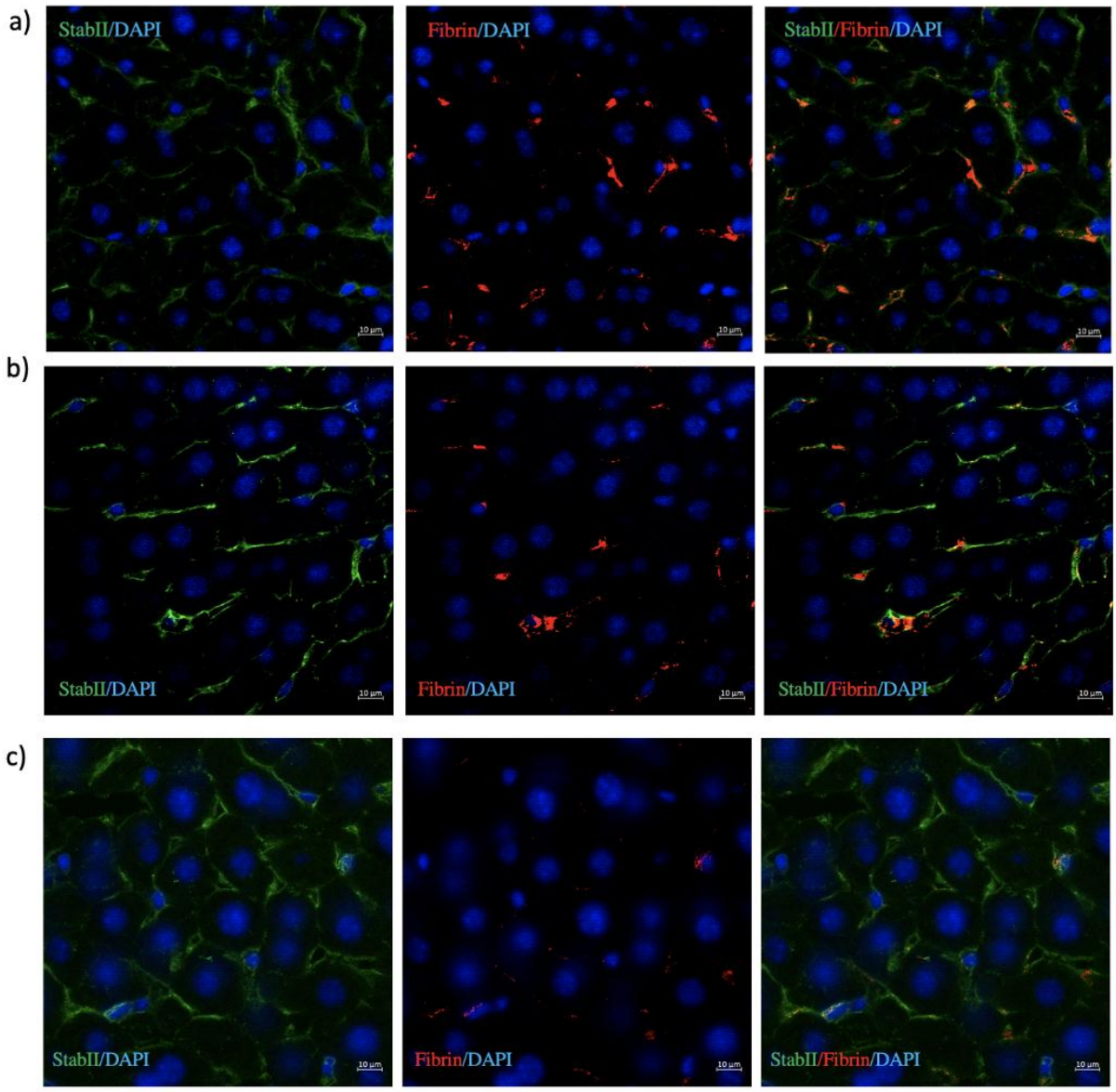
a)
StabII/DAPI
Fibrin/DAPI
StabII/Fibrin/DAPI
b)
StabII/DAPI
Fibrin/DAPI
StabII/Fibrin/DAPI
c)
StabII/DAPI
Fibrin/DAPI
StabII/Fibrin/DAPI

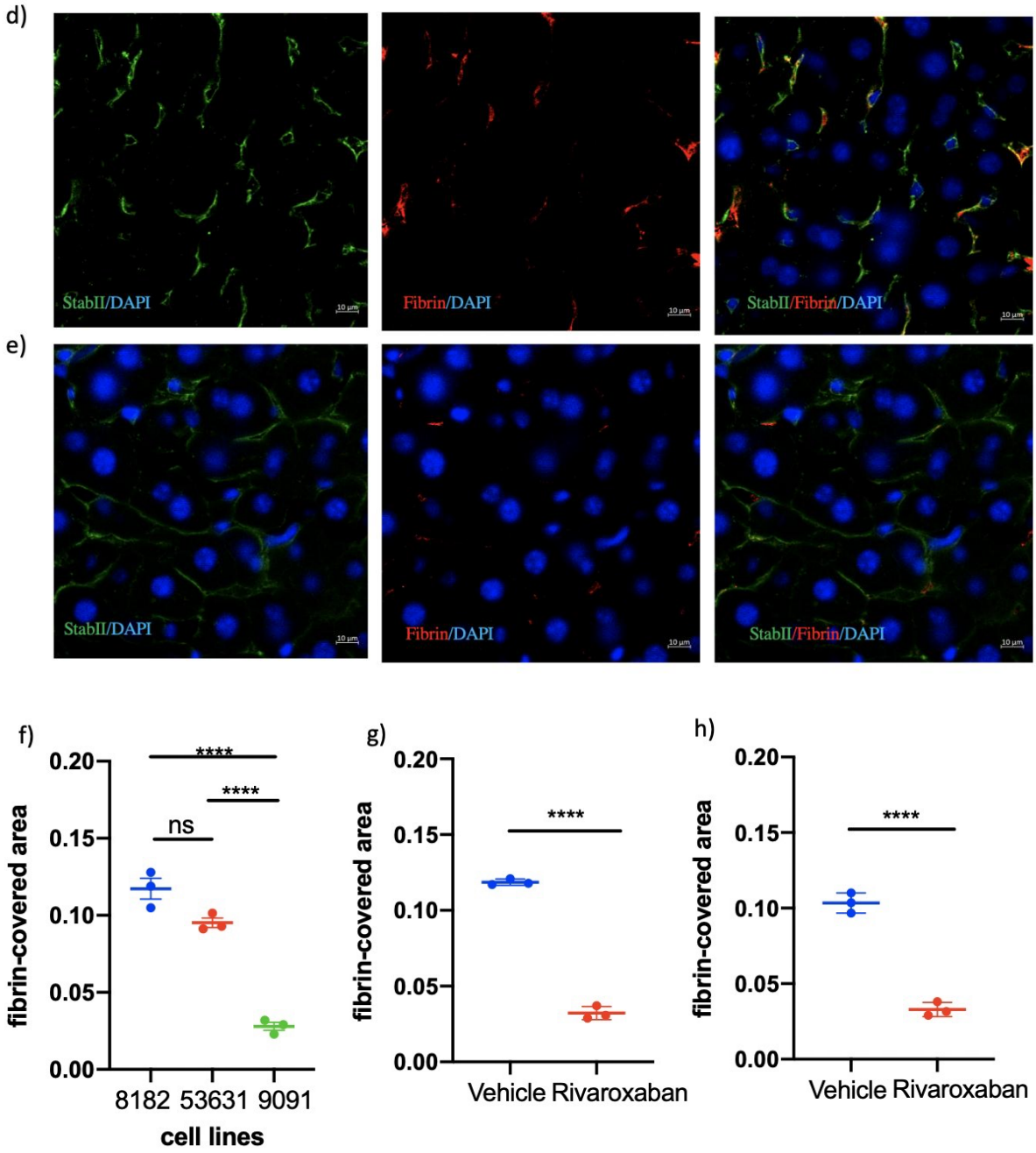

Figure 7 Determination of fibrin formation *in vivo*

a) Representative image indicating fibrin in liver microvessels. Vessels were labeled with Stabilin II (green), and intravascular fibrin was labeled with anti-fibrin antibody (red). Cell line 8182 6 h after injection. Scale bar, 10 µm. **b)** Representative image indicating fibrin in liver microvessels. Vessels were labeled with Stabilin II (green), and intravascular fibrin was labeled with anti-fibrin antibody (red). Cell line 53631 6 h after injection. Scale bar, 10 µm. **c)** Representative image indicating fibrin in liver microvessels. Vessels were labeled with Stabilin II (green), and intravascular fibrin was labeled with anti-fibrin antibody (red). Cell line 9091 6 h after injection. Scale bar, 10 µm. **d)** Representative image indicating fibrin in liver microvessels. Vessels were labeled with Stabilin II (green), and intravascular fibrin was labeled with anti-fibrin antibody (red). DMSO control with cell line 8182 injection. Scale bar, 10 µm. **e)** Representative image indicating fibrin in liver microvessels. Vessels were labeled with Stabilin II (green), and intravascular fibrin was labeled with anti-fibrin antibody (red). Rivaroxaban treatment with cell line 8182 injection. Scale bar, 10 µm. **f)** Quantification of fibrin analysis in the liver microcirculation. The ratio between the area covered by fibrin in the microcirculation and the total microvessel area was calculated. N=3, ns, no significance, ****, P<0.0005 **g)** Quantification of fibrin analysis in the liver microcirculation. Rivaroxaban treated and DMSO control mice were injected with cell line 8182. N=3,

****, P<0.0005. **h)** Quantification of fibrin analysis in liver microcirculation. Rivaroxaban treated and DMSO control mice were injected with cell line 53631. N=3, ****, P<0.0005.

4.1.2 Effect of blood coagulation on the recruitment of non-classical monocytes

Recruitment of non-classical monocytes was determined after injection of the cell lines 8182 and 9091. These two cell lines share high transcriptomic similarities but a tremendous divergence in procoagulant activities both *in vitro* and *in vivo*. Six hours after injection of the cell lines through tail vein, mice were sacrificed, and flow cytometry was conducted to quantify the presence of non-classical monocytes (CD11b+, CD115+, Gr-1-) in the peripheral blood (Figure 8 a, b). Monocyte counts were substantially lower in 9091-injected mice than in 8182-injected mice. The recruitment of non-classical monocytes in the liver microcirculation was lower in mice injected with cell line 9091 than in those injected with cell line 8182 (Figure 8 c). Considering the differences in procoagulant activities between the two cell lines, we hypothesized that fibrin formation was important for recruiting non-classical monocytes. To test this hypothesis, the mice were treated with rivaroxaban. Cell lines 8182 and 53631 were injected into rivaroxaban-treated mice and DMSO control mice. Six hours later, we quantified non-classical monocytes with flow cytometry and in parallel with IHC. After rivaroxaban treatment, significant reductions in blood counts and liver recruitment of non-classical monocytes were observed (Figure 8 d-i). This finding suggested that blood coagulation was a pivotal determinant of non-classical monocyte recruitment in the early phase of metastasis.

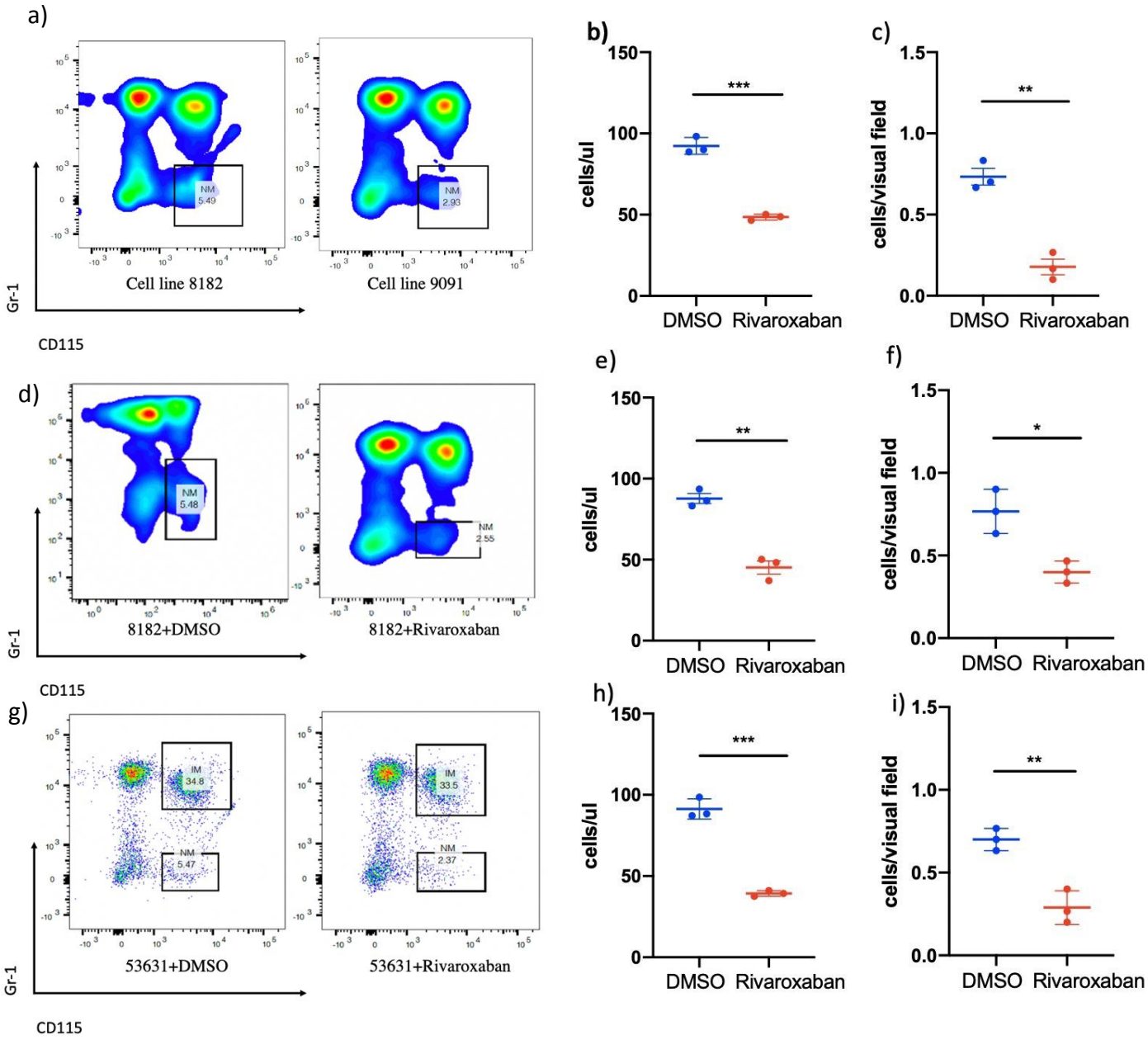

Figure 8 Quantification of non-classical monocyte recruitment

a) Representative gate plot for non-classical monocytes in peripheral blood in mice injected with 8182 or 9091 cells. NM=non-classical monocyte. **b)** Quantification of non-classical monocyte counts in peripheral blood in mice injected with 8182 or 9091 cells. N=3, *** $P < 0.005$. **c)** Non-classical monocyte recruitment in the liver microvessels was quantified by IHC (8182 vs 9091). N=3, ** $P < 0.01$. **d)** Representative gate plot for non-classical monocytes in peripheral blood in rivaroxaban-treated mice injected with cell line 8182. **e)** Quantification of non-classical monocyte counts in peripheral blood in rivaroxaban-treated mice injected with cell line 8182. N=3, ** $P < 0.01$. **f)** Recruitment of non-classical monocytes in the liver microvessels was quantified by IHC. Cell line 8182 was injected into rivaroxaban-treated mice. N=3, * $P < 0.05$. **g)** Representative gate plot for non-classical monocytes in peripheral blood following rivaroxaban-treatment of mice injected with cell line 53631. IM=classical monocyte. **h)** Quantification of non-classical monocyte counts in peripheral blood in rivaroxaban-treated mice injected with cell line 53631. N=3, *** $P < 0.005$. **i)** Recruitment of non-classical monocytes in the liver microvessels was quantified by IHC. Cell line 53631 was injected into rivaroxaban-treated mice. N=3, ** $P < 0.01$.

4.1.3 Interaction of tumor cell EVs with non-classical monocytes

Several studies have shown that non-classical monocytes can engulf EVs (Gordon and Freedman 2006, Yeap, Wong et al. 2017, Robinson, Han et al. 2021). A phenotype screening for EV release indicated that cell line 53631 released the most EVs and had a relatively high ability to recruit non-classical monocytes *in vivo.* PAD4 is responsible for EV release in this cell line (Zhang 2020). Cell line 53631 with downregulated PAD4 expression (53631 PAD4 shRNA) and the respective control cell line (53631 mock shRNA) were injected into mice, and 6 h later, the level of non-classical monocytes in peripheral blood was measured by flow cytometry. In parallel, the liver recruitment of non-classical monocytes was analyzed. Non-classical monocyte counts in peripheral blood and liver recombinant of non-classical monocytes were analyzed. The amounts of non-classical monocytes in peripheral blood (Figure 9 a, b) and in the liver (Figure 9 c) were comparable in both cell lines-transplanted mouse models.

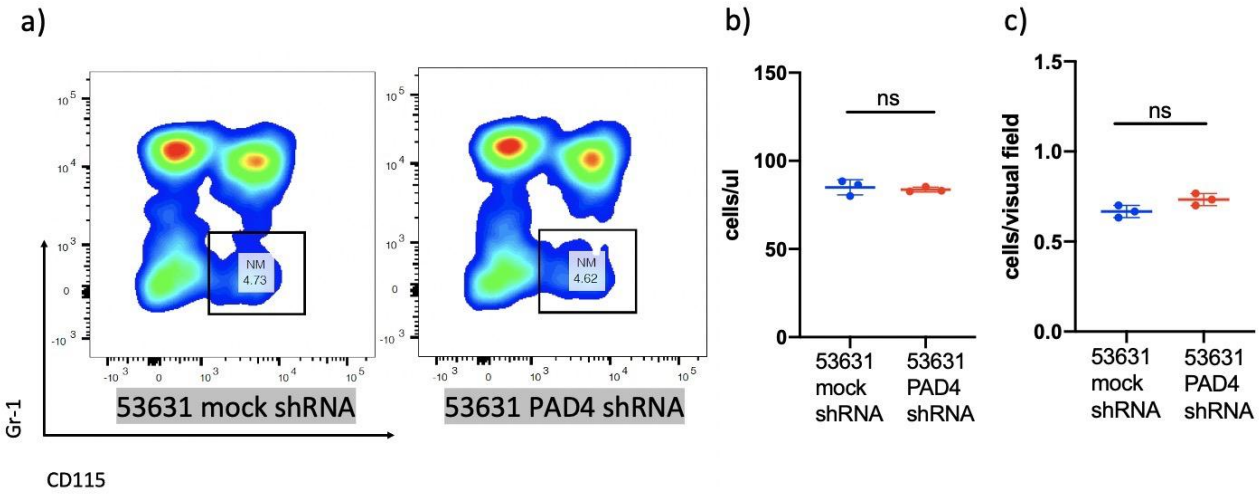

Figure 9 Levels of non-classical monocytes in the presence of tumor cell lines releasing EVs
a) Representative gate plot for non-classical monocytes in the peripheral blood. Mice were injected with cell lines 53631 with mock shRNA or 53631 with PAD4 shRNA. NM=non-classical monocyte. **b)** Levels of non-classical monocytes in peripheral blood. Mice were injected with cell lines 53631 with mock shRNA or 53631 with PAD4 shRNA. N=3; ns, not significant. **c)** Non-classical monocytes in microvessels of the liver were quantified by IHC. Mice were injected with cell line 53631 with mock shRNA or 53631 with PAD4 shRNA. N=3; ns, not significant.

4.1.4 Dependence of the recruitment of non-classical monocytes on fibrin

In mice injected with 8182 cells, the cell line with the highest procoagulant activity, rivaroxaban diminished the recruitment and colocalization of non-classical monocytes with fibrin (Figure 10 a-c). Since the integrin CD11b, which is highly expressed in non-classical monocytes (Ryu, Petersen et al. 2015, Schmid, Khan et al. 2018), can mediate the interaction of immune cells with fibrin (Hernandez, Escolar et al. 1997, Smiley, King et al. 2001), we neutralized CD11b with an anti-CD11b antibody (D'Amico and Wu 2003). Consequently, microvascular fibrin formation and the arrest of non-classical monocytes in the liver microcirculation were quantified. Anti-CD11b antibody did not affect fibrin formation but strongly reduced the recruitment of non-classical monocytes (Figure 10 d, e). Since no significant increase in dead non-classical monocytes was observed in the morphological analysis, this reduction in non-classical monocytes was considered as a decrease in non-classical monocyte recruitment.

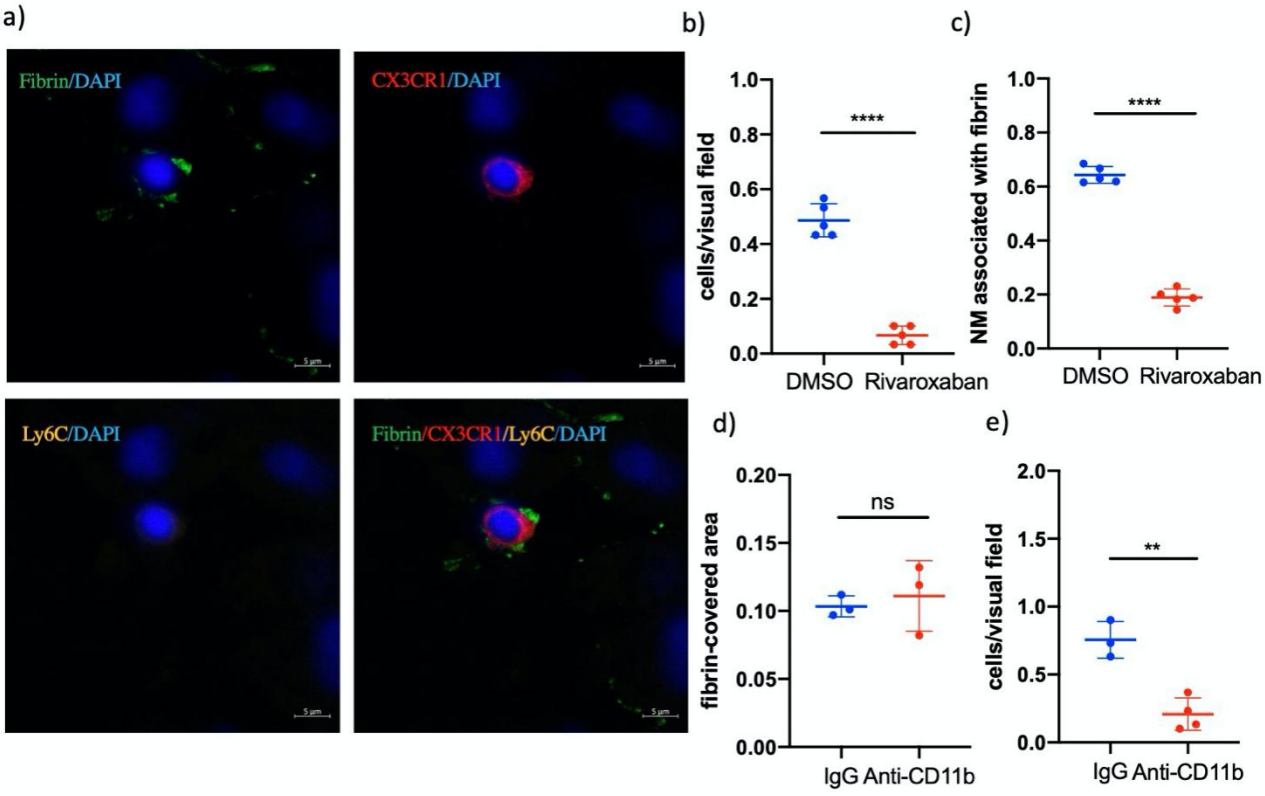

Figure 10 Role of CD11b in the recruitment of non-classical monocytes in the liver microcirculation
a) Representative picture of the colocalization of fibrin (green) with NMs ($CX3CR1^{high}$ $Ly6C^{low}$). Mice injected with cell line 8182. Scale bar, 5 µm. **b)** Colocalization of NMs with fibrin in the liver microcirculation following rivaroxaban treatment. N=5; **** $P < 0.001$. **c)** Ratio of NMs colocalizing with fibrin to total NMs in the liver after rivaroxaban treatment (cell line 8182), N=5; **** $P < 0.001$. **d)** Fibrin formation in the liver microcirculation after application of anti-CD11b neutralizing antibody. N=3; ns, not significant. **e)** Recruitment of NMs after treatment with anti-CD11b antibody. N=3 or 4; ** $P < 0.01$.

4.2 Non-classical monocytes and tumor cell extravasation

4.2.1 Effect of non-classical monocytes on the extravasation of cell line 8182

After injection of anti-CD11b antibody, the extravasation of cell line 8182 was increased. (Figure 11 a, b). To test whether non-classical monocytes could be responsible for this effect, we studied $Nr4a1\_se2^{-/-}$ mice, which exhibit a more specific deficiency in non-classical monocytes than $Nr4a1^{-/-}$ mice (Thomas, Hanna et al. 2016). Flow cytometry was used to determine the number of non-classical monocytes in the peripheral blood and in the liver. Six hours after the injection of cell line 8182, the levels of non-classical monocytes were substantially reduced in $Nr4a1\_se2^{-/-}$ mice compared to WT mice (Figure 11 c-e). Conversely,

the number of Kupffer cells was unchanged (Figure 11 f). To test the effect of non-classical monocytes on tumor cell extravasation, cell line 8182 was injected into Nr4a1_se2$^{-/-}$ mice and WT mice. Six hours after the injection, more tumor cells had extravasated in the Nr4a1_se2$^{-/-}$ mice than in the WT mice, suggesting that NMs could decrease tumor cell extravasation (Figure 11 g). Adoptive transfer of non-classical monocytes obtained from WT mice into Nr4a1_se2$^{-/-}$ mice increased the levels of non-classical monocytes in Nr4a1_se2$^{-/-}$ mice. Concomitantly, tumor cell extravasation was decreased (Figure 11 h, i, j).

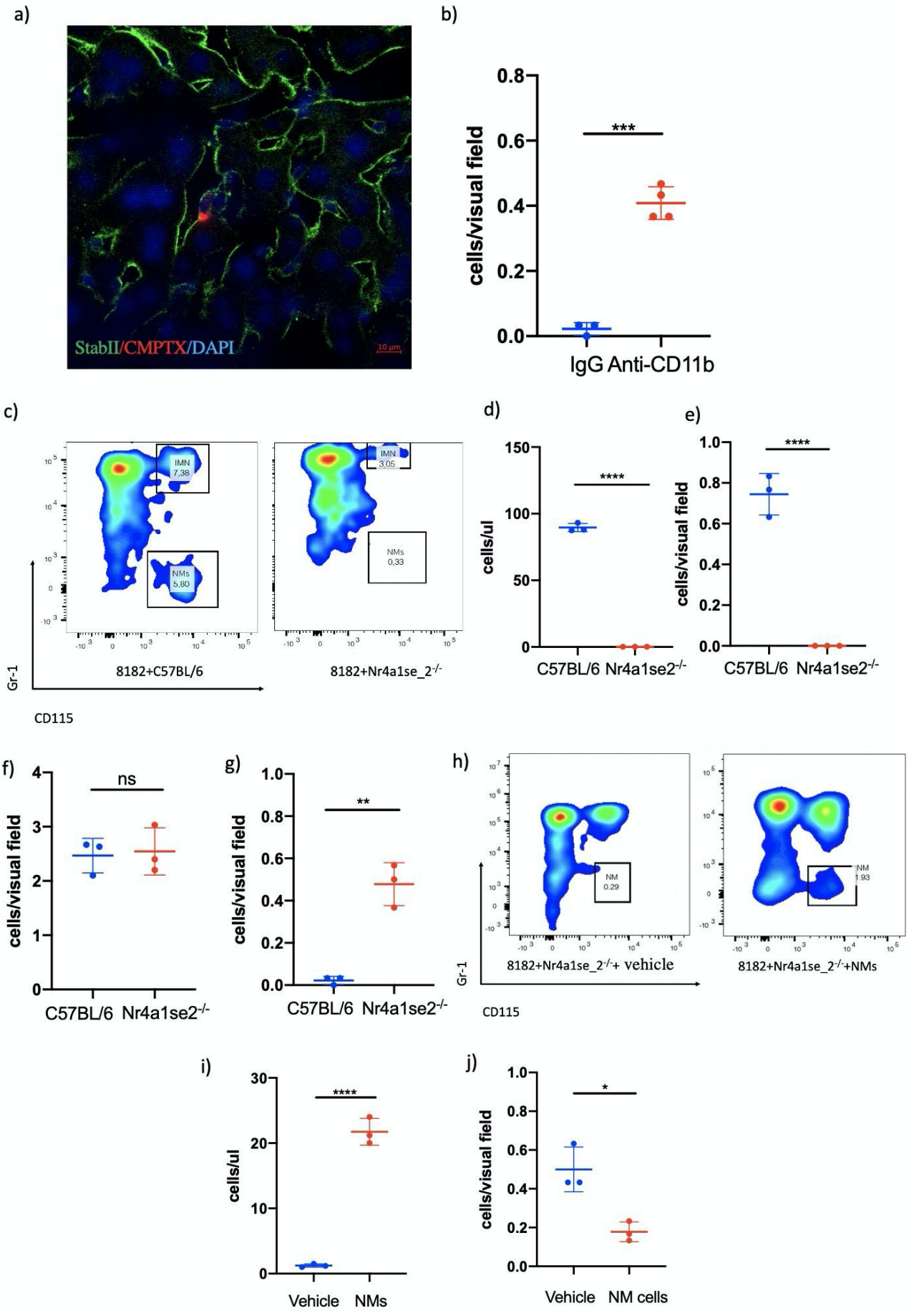
a)
StabII/CMPTX/DAPI
10 µm
b)
cells/visual field
***
IgG Anti-CD11b
c)
IMN 7,38
NMs 5,80
IMN 3,05
NMs 0,33
Gr-1
CD115
8182+C57BL/6
8182+Nr4a1se_2-/-
d)
cells/ul
****
C57BL/6 Nr4a1se2-/-
e)
cells/visual field
****
C57BL/6 Nr4a1se2-/-
f)
cells/visual field
ns
C57BL/6 Nr4a1se2-/-
g)
cells/visual field
**
C57BL/6 Nr4a1se2-/-
h)
NM 0.29
NM 1.93
Gr-1
CD115
8182+Nr4a1se_2-/-+ vehicle
8182+Nr4a1se_2-/-+NMs
i)
cells/ul
****
Vehicle NMs
j)
cells/visual field
*
Vehicle NM cells

Figure 11 Effect of non-classical monocytes on the extravasation of cell line 8182
a) Representative images of the extravasation of cell line 8182. Liver microvessels labeled with Stabilin II (green) and tumor cells prelabeled with CMPTX (red). Scale bar, 10 µm. **b)** Extravasation of cell line 8182 in the presence of anti-CD11b antibody (6 h). N=3, *** $P < 0.005$. **c)** Flow cytometric detection of the levels of non-classical monocytes (CD45+ CD11b+ CD115+ Gr-1-) in the peripheral blood of WT mice and Nr4a1_se2$^{-/-}$ mice injected with cell line 8182. **d)** Quantitative data of the levels of non-classical monocytes in the peripheral blood of Nr4a1_se2$^{-/-}$ mice and WT mice injected with cell line 8182 (flow cytometry). Dots represent different animals. **** $P < 0.0001$. **e)** Quantification of the recruitment of non-classical monocytes in the liver 6 h after 8182 injections in Nr4a1_se2$^{-/-}$ mice and WT mice (8182, 6 h). Dots represent different animals. **** $P < 0.0001$. **f)** Number of Kupffer cells in both Nr4a1_se2$^{-/-}$ mice and WT mice injected with cell line 8182. Dots represent different animals. ns, not significant. **g)** Extravasation of 8182 in WT and Nr4a1_se2$^{-/-}$ mice 6 h after injection. Dots represent different animals. ** $P < 0.01$ **h)** Representative gate plot for non-classical monocytes in peripheral blood following adoptive transfer of WT-derived non-classical monocytes into Nr4a1_se2$^{-/-}$ mice. **i)** Quantification of the levels of non-classical monocytes in peripheral blood 6 h after the adoptive transfer of WT-derived non-classical monocytes in Nr4a1_se2$^{-/-}$ mice. Dots represent different animals **** $P < 0.0001$. **j)** Extravasation of cell line 8182 in Nr4a1_se2$^{-/-}$mice transplanted with WT-derived non-classical monocytes. N=3, * $P < 0.05$.

4.2.2 Role of non-classical monocytes in the extravasation of cell line 53631

Since cell line 8182 exhibited the strongest procoagulant activity and the lowest release of EVs, it represented a good model to specifically study the role of tumor-induced fibrin formation for tumor cell extravasation. Conversely, cell line 53631 strongly induced fibrin formation and exhibited a high release of EVs. Hence, we studied how fibrin formation and non-classical monocytes affected the extravasation of 53631 cells. Rivaroxaban reduced the extravasation of cell line 53631 (Figure 12 a). Moreover, extravasation of 53631 cells was lower in Nr4a1_se2$^{-/-}$ mice (Figure 12 b). Following the adoptive transfer of non-classical monocytes into Nr4a1_se2$^{-/-}$ mice, tumor extravasation of 53631 cells increased (Figure 12 c). Thus, non-classical monocytes potentially facilitated tumor cell extravasation when EVs were present. Since PAD4 is responsible for the release of EVs by cell line 53631, we injected WT mice with 53631 PAD4 shRNA and 53631 mock shRNA cells that differed in their ability to release EVs. The recruitment of immune cells was comparable in both cell lines (Figure 12 d). After treatment with rivaroxaban, recruitment of non-classical monocytes decreased in the presence of both types of 53631 cells (Figure 12 e, f). In WT mice, the extravasation of 53631 PAD4 shRNA cells was reduced compared to the extravasation of 53631 mock shRNA cells. In Nr4a1_se2$^{-/-}$ mice, the extravasation level of both cell lines was comparable (Figure 12 g). This

finding suggested that the interaction of non-classical monocytes with tumor EVs was relevant for tumor cell extravasation.

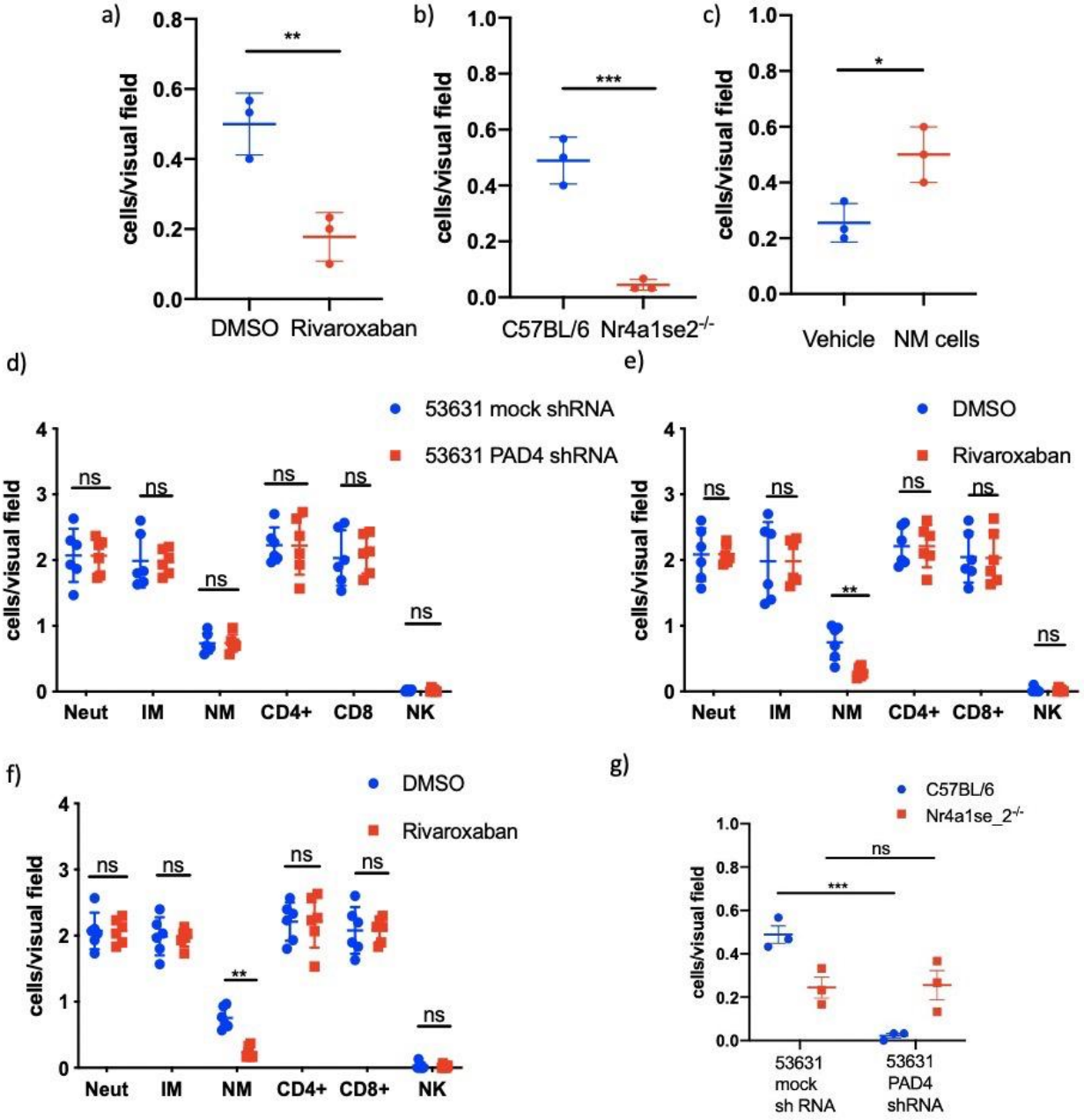

Figure 12 Role of non-classical monocytes in the extravasation of cell line 53631
a) Extravasation of cell line 53631 in rivaroxaban-treated mice (53631, 6 h). n=3, ** P < 0.01. **b)** Extravasation of 8182 cells in WT and Nr4a1_se2$^{-/-}$ mice 6 h after injection. N=3, *** P < 0.005. **c)** Extravasation of cell line 53631 in Nr4a1_se2$^{-/-}$mice receiving adoptive transfer of non-classical monocytes. (53631, 6 h) N=3, * P < 0.05. **d)** Immune cell recruitment in the liver microcirculation was quantified 6 h after injection of cell line 53631 mock shRNA and 53631 PAD4 shRNA cells by IHC. N=6, ns, not significant. Neut, neutrophil; IM, classical monocyte; NM, non-classical monocyte; CD4+, CD4+ T cell; CD8, CD8+ T cells; NK, natural killer cell. **e)** Immune cell recruitment in the liver microcirculation in rivaroxaban-treated mice (53631 mock shRNA cells, 6 h). N=6, ** P < 0.01, ns, not significant. **f)** Immune cell recruitment in the liver microcirculation in rivaroxaban-treated mice

(53631 PAD4 shRNA cells, 6 h). N=6, ** P < 0.01, ns, not significant. **g)** Extravasation of 53631 mock shRNA and 53631 PAD4 shRNA cells in WT and Nr4a1_se2$^{-/-}$ mice (6 h). N=3, *** P < 0.005, ns, not significant.

4.3.1 Potential mechanism underlying the role of non-classical monocytes in the extravasation of cell line 8182

Given the participation of the Ang-1/Ang-2 system in endothelial barrier function, we analyzed the expression of Ang-1 in neutrophils, classical monocytes, non-classical monocytes, CD4+ T cells, CD8+ T cells, NK cells, and Kupffer cells in the liver and evaluated the effect of rivaroxaban. Ang-1 was mostly associated with non-classical monocytes (Figure 13 a). Rivaroxaban reduced the number of Ang-1^{+} non-classical monocytes (Figure 13 b). No Ang-2 was detected in the recruited immune cells (Figure 13 c). Flow cytometry of non-classical monocytes in the peripheral blood was applied to quantify those expressing Ang-1 and Ang-2. This analysis confirmed the percentage of high counts of Ang-1-positive non-classical monocytes, whereas the association of Ang-2 was very low. Rivaroxaban strongly diminished Ang-1-positive non-classical monocytes but did not affect Ang-2 expression (Figure 13 d-g). After CD11b neutralization, the number of non-classical monocytes was reduced dramatically, especially the number of Ang-1^{+} non-classical monocytes (Figure 13 h, i).

The high expression of Ang-1 in non-classical monocytes could contribute to the inhibition of tumor cell extravasation by these cells. To test whether fibrin could regulate the expression of Ang-1 in non-classical monocytes, isolated non-classical monocytes were exposed to fibrin for 4 h *in vitro*. Flow cytometry results and western blotting showed that fibrin enhanced Ang-1 expression in non-classical monocytes (Figure 13 j-m). Six hours after injection of 8182 cells and treatment with rivaroxaban, non-classical monocytes were extracted from the mice. After treatment with rivaroxaban, Ang-1 expression in non-classical monocytes decreased sharply (Figure 13 n-q). Together, these results indicate that the interaction between non-classical monocytes and fibrin *in vivo* and *in vitro* increased the Ang-1 expression in these cells.

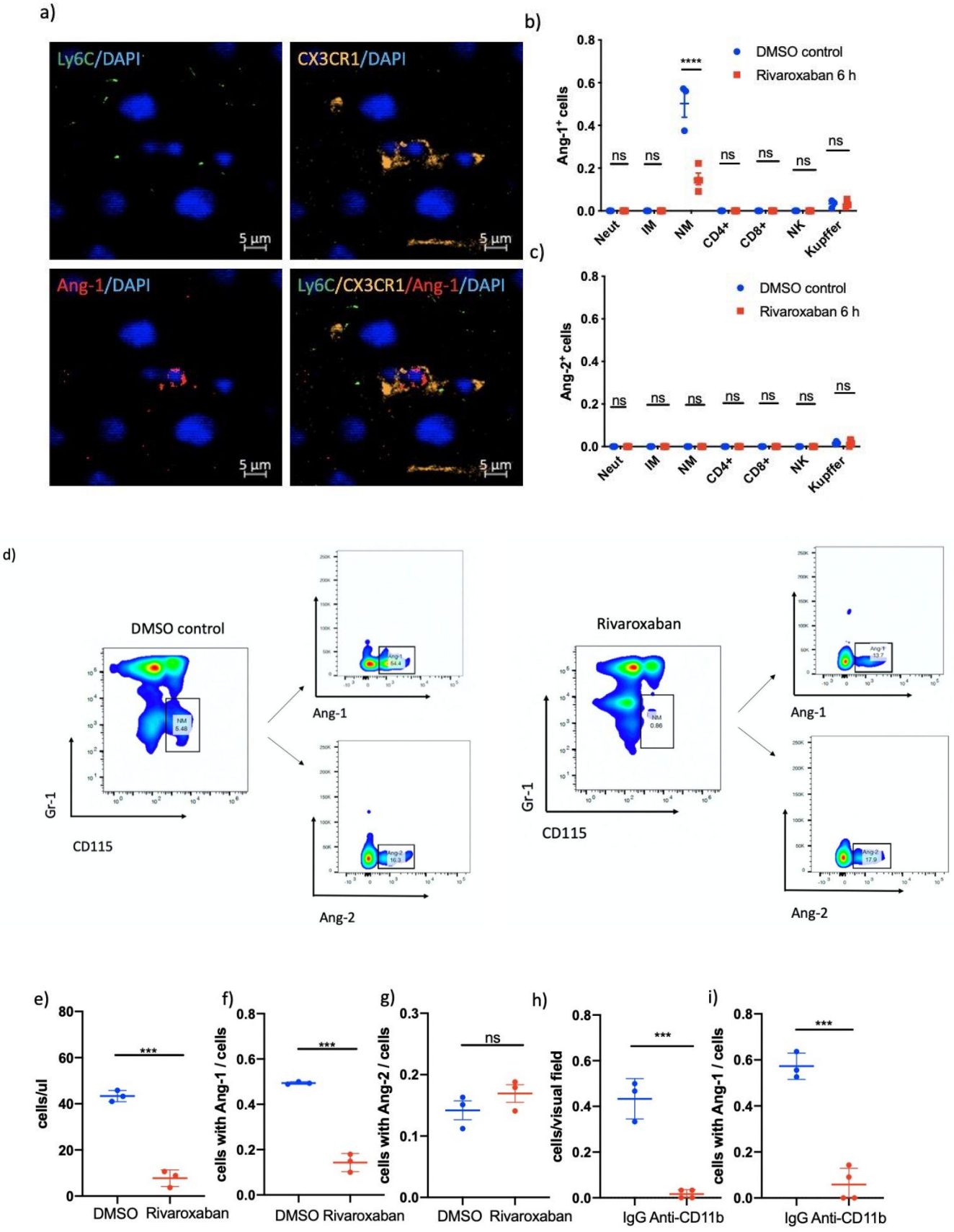
a)
Ly6C/DAPI
CX3CR1/DAPI
Ang-1/DAPI
Ly6C/CX3CR1/Ang-1/DAPI
5 µm
b)
DMSO control
Rivaroxaban 6 h
Ang-1+ cells
****
ns
Neut
IM
NM
CD4+
CD8+
NK
Kupffer
c)
Ang-2+ cells
d)
DMSO control
Rivaroxaban
Gr-1
CD115
Ang-1
Ang-2
e)
cells/ul
***
DMSO
Rivaroxaban
f)
cells with Ang-1 / cells
g)
cells with Ang-2 / cells
h)
cells/visual field
IgG Anti-CD11b
i)

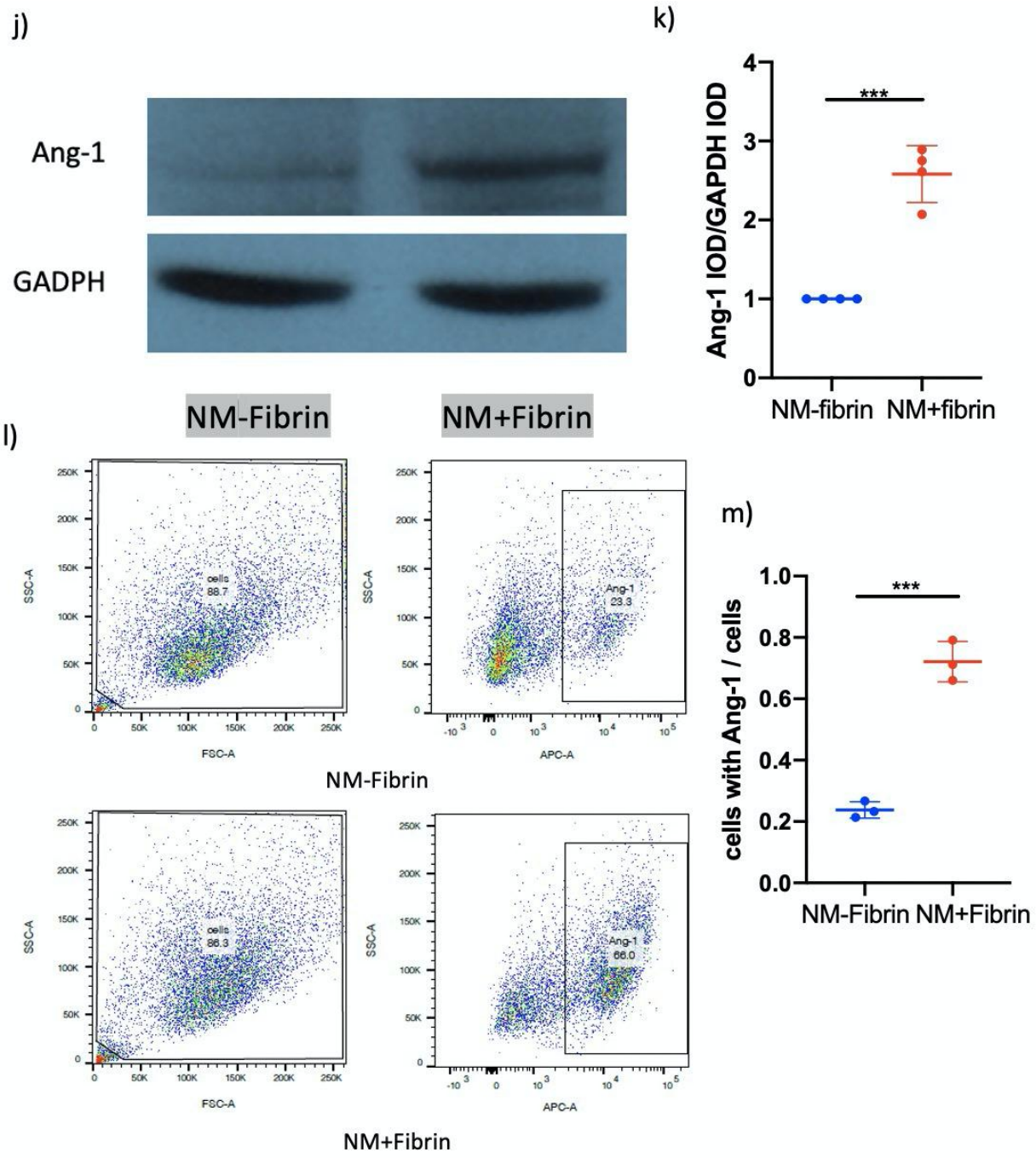
j)
Ang-1
GADPH
k)
Ang-1 IOD/GAPDH IOD
***
NM-fibrin
NM+fibrin
l)
NM-Fibrin
NM+Fibrin
SSC-A
FSC-A
cells
88.7
Ang-1
23.3
APC-A
NM-Fibrin
cells
86.3
Ang-1
66.0
NM+Fibrin
m)
cells with Ang-1 / cells
***
NM-Fibrin
NM+Fibrin

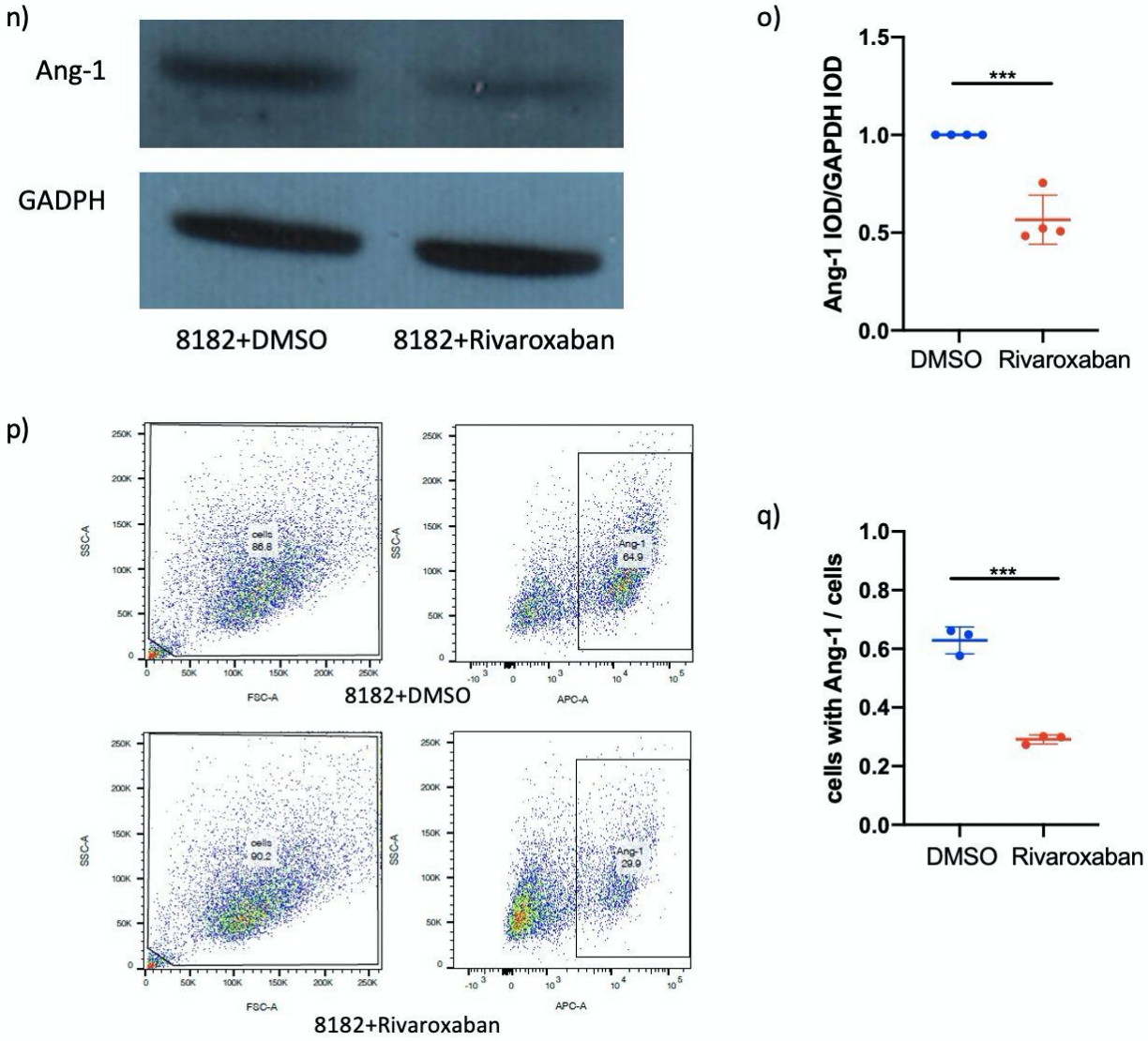

Figure 13 Potential mechanism allowing non-classical monocytes to impede 8182 cell extravasation
a) Representative images of non-classical monocytes (CX3CR1high Ly6Clow) expressing Ang-1 in the liver. Ly6C (green) CX3CR1 (orange), Ang-1 (red), DAPI (blue). Scale bar, 5 µm. **b)** Immune cells positive for Ang-1 after rivaroxaban treatment (8182, 6 h). N=3. ****P < 0.001, ns not significant. **c)** Association of Ang-2 with immune cells after rivaroxaban treatment (8182, 6 h). N=3. ns, not significant. **d)** Representative gate plot for Ang-1 or Ang-2 with non-classical monocytes in the peripheral blood 6h after injection of cell line 8182 without or with rivaroxaban. **e)** Quantification of Ang-1 positive non-classical monocytes in the peripheral blood in rivaroxaban-treated mice. N=3. *** P < 0.005. **f)** Ratios of non-classical monocytes expressing Ang-1 to total non-classical monocytes in rivaroxaban-treated mice (peripheral blood). N=3. *** P < 0.005. **g)** Ratios of non-classical monocytes associated with Ang-2 to total non-classical monocytes in rivaroxaban-treated mice (peripheral blood). N=3. ns, not significant. **h)** Recruitment of non-classical monocytes in mice treated with anti-CD11b neutralizing antibody. N=3. *** P < 0.005. **i)** Ratios of Ang-1 positive non-classical monocytes to total non-classical monocytes in mice treated with anti-CD11b neutralizing antibody. N=3. *** P < 0.005. **j)** Representative WB of Ang-1 and GAPDH (housekeeping) in non-classical monocytes without and with co-incubation with fibrin *in vitro*. **k)** Densitometric quantification of WB analyses *in vitro*. N=4, **** P < 0.001. **l)** Representative gate plot of Ang-1 positive non-classical monocytes without or with co-incubation with fibrin *in vitro*. **m)** Quantitative data of non-classical monocytes expressing Ang-1 with and without co-incubation with fibrin *in vitro* based on flow cytometry. N=3. *** P < 0.005. **n)** Representative WB of Ang-1 and GAPDH (housekeeping) in non-classical monocytes after treatment of rivaroxaban. **o)** Densitometric quantification of WB

analyses *in vivo*. N=4, *** P < 0.005. **p)** Representative gate plot of Ang-1 positive non-classical monocytes in rivaroxaban-treated mice. q) Quantitative data of Ang-1 positive non-classical monocytes after treatment with rivaroxaban. N=3, *** P < 0.005.

4.3.2 Potential mechanism underlying the role of non-classical monocytes in the extravasation of cell line 53631.

Non-classical monocytes thus appear to play different roles in tumor cell extravasation of cell lines 8182 and 53631. Since these two cell lines greatly differ in EV release levels, we considered that EVs might be relevant for the extravasation of 53631. Following the injection of 53631 mock shRNA and 53631 PAD4 shRNA cells, the expression of Ang-1 and Ang-2 in non-classical monocytes was analyzed in the liver microcirculation. The number of Ang-1-positive non-classical monocytes was higher after 53631 PAD4 shRNA cell injection than after 53631 mock shRNA cell injection (Figure 14 a). In contrast, Ang-2 expression was lower in non-classical monocytes after injection with cell line 53631 PAD4 shRNA than after injection with 53631 mock shRNA cells (Figure 14 b). Similar results were observed with IHC and flow cytometry (Figure 14 c-g).

The high association between Ang-2 expression and non-classical monocytes could facilitate tumor cell extravasation. To test whether EVs could be responsible for Ang-2 expression in non-classical monocytes, isolated non-classical monocytes were co-incubated for 4h with tumor-derived EVs *in vitro*. Flow cytometry and western blotting showed that EVs increased the number of Ang-2-positive non-classical monocytes (Figure 14 h-k). Non-classical monocytes were isolated 6 h after injection of 53631 mock shRNA or 53631 PAD4 shRNA cells. In mice injected with 53631 PAD4 shRNA cells, the number of non-classical monocytes expressing Ang-2 was significantly lower than after administration of 53631 mock shRNA cells (Figure 14 l-o). Together, these results indicate that the interaction between non-classical monocytes and tumor EVs *in vivo* and *in vitro* increases their Ang-2 positivity rate.

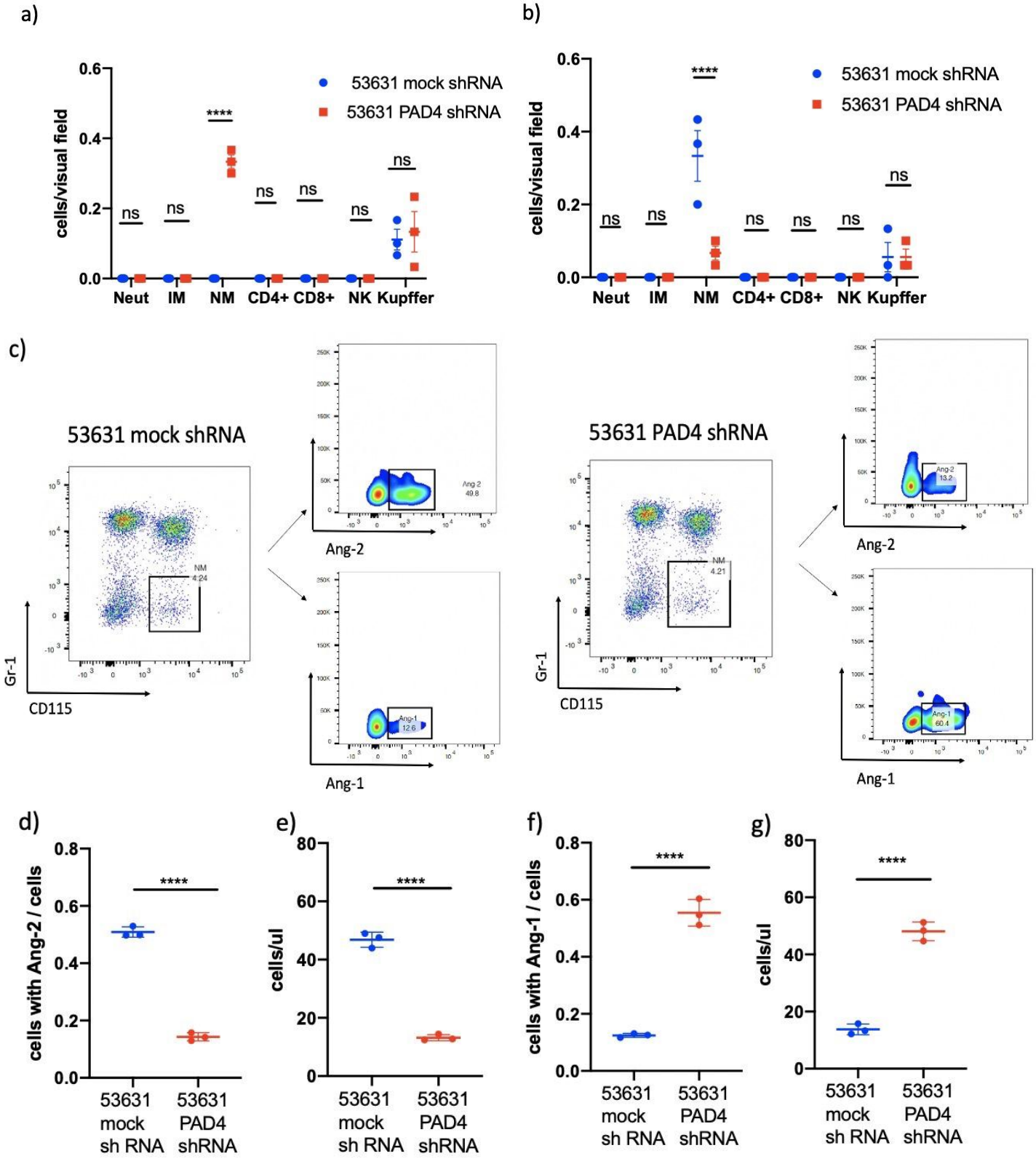
a)
b)
cells/visual field
53631 mock shRNA
53631 PAD4 shRNA
****
ns
Neut
IM
NM
CD4+
CD8+
NK
Kupffer
c)
53631 mock shRNA
53631 PAD4 shRNA
Gr-1
CD115
NM
4.24
4.21
Ang-2
Ang-1
Ang-2 49.8
Ang-2 13.2
Ang-1 12.6
Ang-1 60.4
d)
e)
f)
g)
cells with Ang-2 / cells
cells with Ang-1 / cells
cells/ul
53631 mock sh RNA
53631 PAD4 shRNA

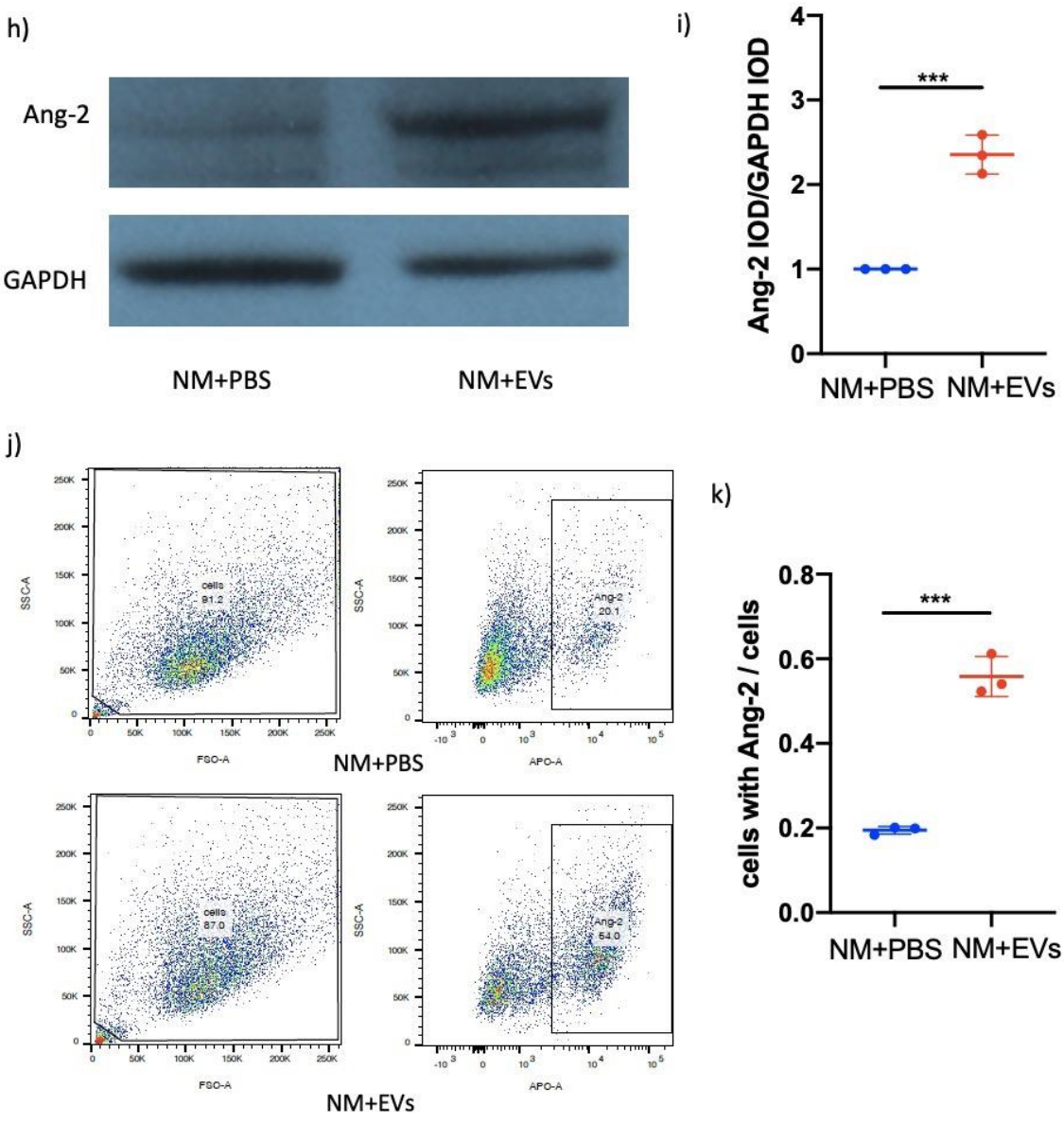
h)
Ang-2
GAPDH
NM+PBS
NM+EVs
i)
Ang-2 IOD/GAPDH IOD
***
NM+PBS
NM+EVs
j)
SSC-A
FSC-A
cells
91.2
Ang-2
20.1
APC-A
NM+PBS
cells
87.0
Ang-2
64.0
NM+EVs
k)
cells with Ang-2 / cells
***
NM+PBS
NM+EVs

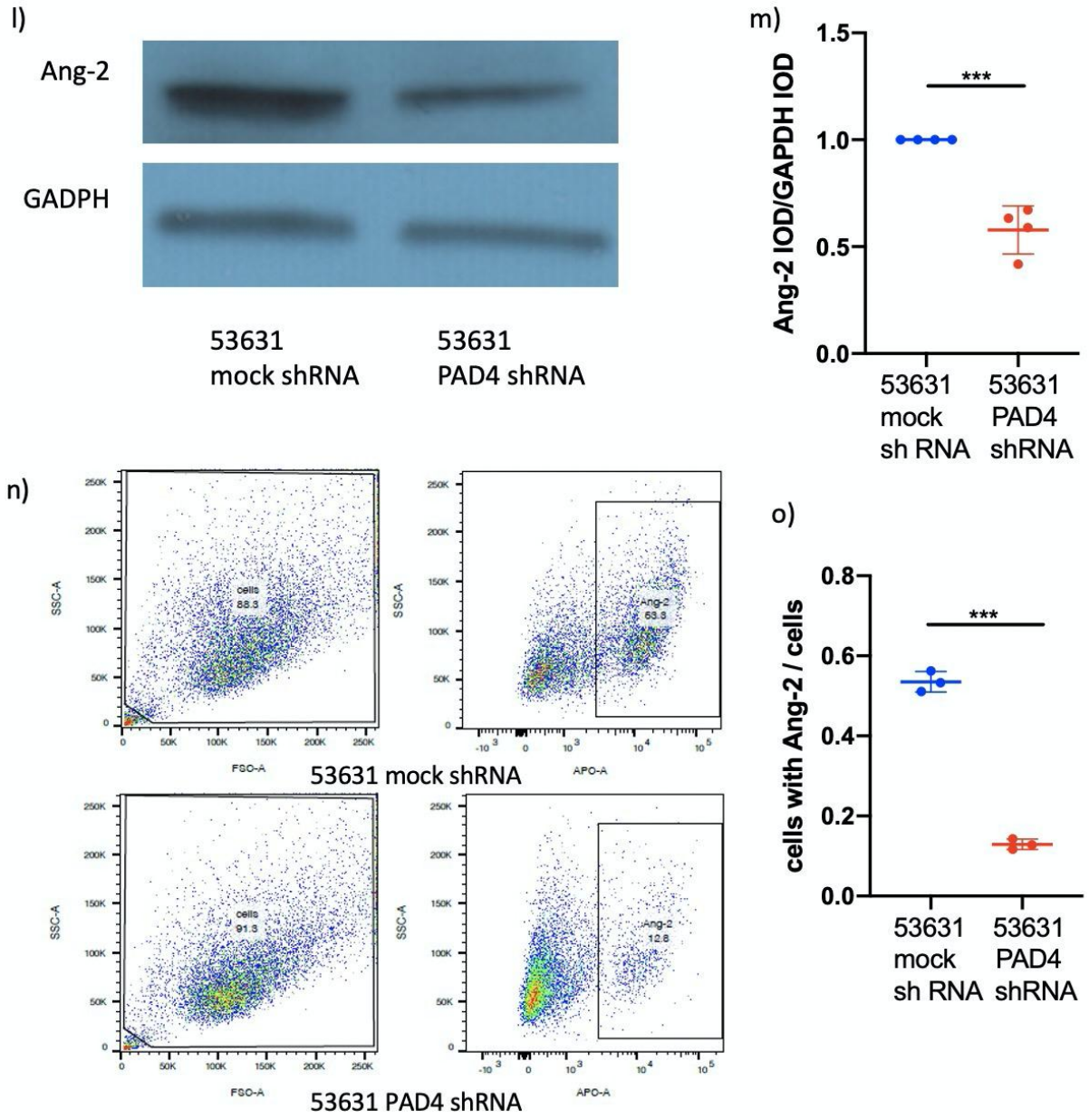

Figure 14 Ang-1 and Ang-2 expression in non-classical monocytes in the presence of tumor cells releasing EVs

a) Ang-1$^+$ immune cells 6 h after injection of 53631 mock shRNA or 53631 PAD4 shRNA tumor cells. N=3, ns, not significant, **** P < 0.001. Neut, neutrophil, IM, classical monocyte, NM, non-classical monocyte, CD4+, CD4+ T cell, CD8+, CD8+ T cells, NK, natural killer cell. **b)** Ang-2$^+$ immune cells 6 h after injection of 53631 mock shRNA or 53631 PAD4 shRNA tumor cells. N=3, ns, not significant, **** P < 0.001. **c)** Representative gate plot for Ang-1 and Ang-2 positivity of non-classical monocytes in peripheral blood 6 h after injection of 53631 mock shRNA or 53631 PAD4 shRNA cell lines. **d)** Ratios of Ang-2$^+$ non-classical monocytes to total non-classical monocytes 6 h after injection of 53631 mock shRNA or 53631 PAD4 shRNA cells (peripheral blood). N=3, **** P < 0.001 **e)** Quantification of Ang-2$^+$ non-classical monocytes in the peripheral blood 6 h after injection of 53631 mock shRNA or 53631 PAD4 shRNA cell lines. N=3, **** P < 0.001. **f)** Ratios of Ang-1$^+$ non-classical monocytes to total non-classical monocytes 6 h after injection of 53631 mock shRNA or 53631 PAD4 shRNA cell lines (peripheral blood). N=3, **** P < 0.001. **g)** Quantification of Ang-1$^+$ non-classical monocytes in the peripheral blood 6 h after injection of 53631 mock shRNA or 53631 PAD4 shRNA cells. N=3, **** P < 0.001. **h)** Representative WB of Ang-2 association with non-classical monocytes following incubation with tumor EVs *in vitro*. **i)** Densitometric quantification of WB analyses showing in Figure 14 h. N=4, *** P < 0.005. **j)** Representative gate plot of Ang-2$^+$ non-classical monocytes following incubation with tumor EVs *in vitro*. **k)** Quantitation of data of Figure 14 j. N=3. *** P < 0.005. **l)** Representative WB of Ang-2 association with

non-classical monocytes 6 h after injection of 53631 mock shRNA or 53631 PAD4 shRNA cell lines. **m)** Quantification of the results shown in Figure 14 l. N=4, *** $P < 0.005$. **n)** Representative gate plot of Ang-2^+ non-classical monocytes 6 h after injection of 53631 mock shRNA or 53631 PAD4 shRNA cell lines. **o)** Quantitation of the results of Figure 14 n. N=3, *** $P < 0.005$.

5. Discussion

1. Role of blood coagulation in the recruitment of non-classical monocytes

In a previous study, a total of 11 PDAC cell lines with the $Kras^{G12D}$ mutation were selected for procoagulant screening. The results showed that cell lines 8182 and 53631 had the strongest procoagulant activities. Conversely, cell line 9091 had the weakest procoagulant activity. In this study, we first sought to determine the role of coagulation in the recruitment of non-classical monocytes. Rivaroxaban, a direct FXa inhibitor used clinically as an anticoagulant, was administered to inhibit fibrin formation (Kopytek, Zabczyk et al. 2019). After rivaroxaban administration, fibrin formation in cell lines 8182 and 53631 decreased by over 70% compared to the control group. In separate experiments, we analyzed the recruitment of non-classical monocytes in animals injected with cell lines 8182 and 9091. We noted that recruitment of non-classical monocytes sharply decreased in mice injected with cell line 9091 compared to in those injected with cell line 8182. After injection of rivaroxaban, the arrest of non-classical monocytes was reduced in animals administered cell lines 8182 and 53631 compared to the DMSO control group. This finding suggested that blood coagulation is a pivotal factor in inducing the recruitment of non-classical monocytes and that fibrin can arrest non-classical monocytes.

Monocytes are innate immune cells of the mononuclear phagocyte system. Substantial evidence indicates that monocytes could be vital regulators of cancer progression and development (Olingy, Dinh et al. 2019, Gouveia-Fernandes 2020). For instance, Chen et al. revealed that peritumoral monocytes induce cancer cell autophagy to facilitate the progression of human hepatocellular carcinoma (Chen, Ning et al. 2018). Moreover, some studies have revealed that non-classical monocytes can engulf EVs to increase tumor cell spread (Yona and Jung 2010, Himes, Peterson et al. 2020). Hence, we aimed to clarify the

role of non-classical monocytes and their interactions with EVs during the early stage of pancreatic cancer metastasis. Previously, it has been shown that the release of EVs is reduced in cell line 53631 when the expression of the PAD4 gene is reduced. Interestingly, knockdown of PAD4 by shRNA did not affect the recruitment of non-classical monocytes.

Several studies have revealed that fibrin is a ligand for the integrin CD11b expressed by myeloid cells. Immune cells can be activated by the interaction between CD11b and fibrin (Perez and Roman 1995, Zhang, Yin et al. 2020). Although this activation mechanism has been reported to be relevant in cancer, the immune cells involved were not non-classical monocytes (Zhang, Ozdemir et al. 2011, Ozdemir, Zhang et al. 2012). Since non-classical monocytes patrol and surveil endothelial cells, these cells could potentially detect tumor-induced fibrin. Indeed, we observed colocalizations between fibrin clots and non-classical monocytes in the liver microcirculation following the immobilization of the tumor cells. Therefore, we hypothesized that CD11b might function as a crucial mediator between non-classical monocyte recruitment and coagulation in cancer. Following injection of anti-CD11b antibody, the arrest of non-classical monocytes was greatly diminished. Fibrin formation was not affected.

2. Role of non-classical monocytes in PDAC cell extravasation

Tumor cell extravasation is a key step in the metastasis cascade, which requires interaction between tumor cells and the endothelium (Desch, Strozyk et al. 2012). Therefore, blocking tumor cell extravasation is critical for inhibiting tumor metastasis, and exploring the possible underlying mechanisms of extravasation is important. CD11b was neutralized to analyze whether non-classical monocytes affect tumor cell extravasation, and the

extravasation of cell line 8182 was increased. This finding suggested that tumor-induced recruitment of non-classical monocytes could hinder tumor cell extravasation.

In addition, a mouse model in which non-classical monocytes are largely absent owing to the pivotal effect of Nr4a1 on the differentiation of lymphocyte antigen 6C (Ly6C)-high monocytes into Ly6C-low monocytes was studied (Bharat, McQuattie-Pimentel et al. 2017, Prabowo, Painter et al. 2019, Zhang 2020, Ren, Li et al. 2021). Specifically, we used Nr4a1_se2$^{-/-}$ mice, which exhibit a more specific deficiency in non-classical monocytes than Nr4a1$^{-/-}$ mice due to the deletion of a Nr4a1 super-enhancer (Thomas, Hanna et al. 2016). Parallel to the massive reduction in non-classical monocytes in this mouse model, extravasation of the tumor cell line 8182 was increased in the Nr4a1_se2$^{-/-}$ mice compared to WT mice. This finding indicated that non-classical monocytes could decrease the extravasation of cell line 8182. Furthermore, the adoptive transfer of non-classical monocytes into Nr4a1_se2$^{-/-}$ mice decreased the extravasation of the tumor cells, further indicating that non-classical monocyte could inhibit 8182 tumor cell extravasation.

EVs coordinate multiple systemic pathophysiological processes, such as coagulation, vascular leakage and reprogramming of stromal cells, to support the pre-metastatic niche formation and subsequent metastasis (Becker, Thakur et al. 2016, Headley, Bins et al. 2016, Pfeiler, Thakur et al. 2019). Since cell line 53631 strongly induced fibrin formation and exhibited a high release of EVs, we used this cell line to study how fibrin formation and non-classical monocytes contribute to tumor cell extravasation. We found that rivaroxaban reduced the extravasation of tumor cell line 53631. Interestingly, the extravasation of 53631 cells was lower in Nr4a1_se2$^{-/-}$ mice than in WT mice. Conversely, tumor extravasation of 53631 cells was increased after the adoptive transfer of non-classical monocytes into

Nr4a1_se2$^{-/-}$ mice. Hence, contrary to observations made with cell line 8182, non-classical monocytes increased the extravasation of cell line 53631. Thus, we suspected that non-classical monocytes potentially facilitate tumor cell extravasation when EVs are present. To confirm the role of EVs, we injected PAD4 shRNA-transfected 53631 cells into WT mice to evaluate the arrest of non-classical monocyte recruitment and tumor cell extravasation. The results showed that the 53631 mock shRNA cell line released a large level of EVs *in vivo*, whereas the 53631 PAD4 shRNA cell line released a comparably low level, similar to the results obtained in the *in vitro* experiments. Moreover, regarding tumor cell extravasation, mock shRNA-transfected 53631 cells extravasated significantly more than PAD4 shRNA-transfected 53631 cells. Overall, the results obtained above indicated that non-classical monocytes can play dual roles in tumor cell extravasation and that their effect is EV-dependent. When EVs are absent, non-classical monocytes impede tumor cell extravasation, whereas these cells facilitate tumor cell extravasation when EVs are present.

3. *Potential mechanisms underlying the differential roles of non-classical monocytes in tumor cell extravasation*

Angiopoietins, such as Ang-1 and Ang-2, have a wide range of effects on tumor malignancy via their effect on angiogenesis, inflammation, and extravasation (Shim, Ho et al. 2007). Ang-1 supports endothelial stabilization via Tie2 activation, which is an important regulator of tumor cell extravasation (Suri, Jones et al. 1996, Jeansson, Gawlik et al. 2011). Ang-2 functions as a context-dependent Tie2 agonist/antagonist promoting pathological angiogenesis, vascular permeability and inflammation (Maisonpierre, Suri et al. 1997, Daly, Eichten et al. 2013). In addition, previous studies have revealed that overexpression of Ang-1 in some cancer types significantly inhibits metastasis, including the metastasis of breast cancer (Hayes, Huang et al. 2000), colon cancer (Stoeltzing, Ahmad et al. 2003), and

squamous cell carcinoma (Hawighorst, Skobe et al. 2002). The inhibitory effect of Ang-1 is related to the recruitment of perivascular cells that restrict further expansion of the tumor vasculature. Other evidence has shown that Ang-2 overexpression is related to tumor growth, metastasis and malignancy (Tanaka, Mori et al. 1999, Ahmad, Liu et al. 2001, Etoh, Inoue et al. 2001). Therefore, we investigated whether Ang-1 and Ang-2 participated in the dual roles of non-classical monocytes in tumor cell extravasation. We found that Ang-1 was expressed only in non-classical monocytes among the intravascular cells. Rivaroxaban reduced the number of Ang-1+ non-classical monocytes but did not affect the number of Ang-2+ non-classical monocytes *in vivo* or *in vitro*. This finding suggested that the interaction of non-classical monocytes with fibrin might increase the Ang-1 expression in non-classical monocytes, thereby attenuating tumor cell extravasation.

To understand why EVs released by 53631 cells could alter the ability of non-classical monocytes to inhibit tumor cell extravasation, we focused our attention on Ang-2. Thus, cell line 53631 was utilized to analyze the effect of EVs and whether Ang-2 was involved in the adverse effect of non-classical monocytes on tumor cell extravasation. We found that compared to in animals injected with the mock shRNA-transfected 53631 cells, the number of Ang-2+ non-classical monocytes was decreased in animals injected with PAD4 shRNA-transfected 53631 cells; a similar effect was observed *in vitro*. In addition, we found that EVs enhanced the number of Ang-2+ non-classical monocytes *in vitro* and *in vivo*. This finding suggested that the interaction between non-classical monocytes and tumor cell EVs increased monocyte Ang-2 expression, likely facilitating tumor cell extravasation.

4. Limitations of this study

Several limitations of this study must be addressed. Even though procoagulant screening via TEG was performed in 11 different cell lines previously, only 3 cell lines with prominent procoagulant activity were studied here. Therefore, all conclusions in this study should be considered preliminary, and more experiments are required to validate and solidify the conclusions presented in this thesis. Moreover, all cell lines utilized in this study were mouse-derived PDAC cell lines. Thus, our conclusions are based on the animal experiments, which represents a limitation in the translational value of the study. Subsequent clinical trials and research studies are required to elucidate the value of anticoagulant therapy for pancreatic cancer patients.

To validate that fibrin formation-induced non-classical monocytes recruitment was mediated by CD11b, a CD11b neutralizing antibody was administered. As CD11b is a member of the integrin family of cell adhesion receptors expressed in several immune cells, the effect of the CD11b neutralizing antibody was comprehensive. More precise methods could be developed, such as establishing conditional knock-out mice.

The Nr4a1_se2$^{-/-}$ mouse strain was employed to unveil the role of non-classical monocytes in pancreatic cancer cell extravasation. After the deletion of an Nr4a1 super-enhancer subdomain in this strain, Ly6C^{low} monocyte numbers were significantly decreased with preservation of macrophage gene function. While this model is not perfect, it is widely accepted and used in the field of non-classical monocytes research. Adoptive monocyte transplantation was performed to confirm our observations.

6. Figure list

7. Publications related to this thesis

1. Detection of molecular signatures and pathways shared in ulcerative colitis and colorectal cancer using a bioinformatics approach (submitted)
   Xiaopeng Zhang*, Can Lu*, Weibin Wang

2. Coagulation-mediated immune cells function in pancreatic cancer early metastasis (In preparation)
   Xiaopeng Zhang*, Hellen Ishikawa-Ankerhold*, Manoviriti Thakur, Mona Wohlrab, Maximilian Wieser, Martina Reiser, Michael Völkl, Magdalena Berchtold, Kathrin Gärtner, Christian Schulz, Steffen Massberg, Roland Rad, Bernd Engelmann

3. Concerted control of blood coagulation and T helper cells in intravascular infections (submitted)
   Tonina T Mueller*, Manoviriti Thakur*, Mona Wohlrab*, Sarah Meister, Flavio Karaj, Laura Garcia Perez, Rupert Öllinger, Thomas Engleitner, Torben LangHeinrich, Micheal Völkl, Xiaopeng Zhang, Claudia Tersteeg, Matthias Mack, Uwe Koedel, Alexandar Zigman Kohlmaier, Daniel Teupser, Philipp von Hundelshausen, Christian Weber, Christian Schulz, Sabrina Bortoluzzi, Jürgen Bernhagen, Klaus T. Preissner, Roland Rad, Marc Schmidt-Supprian, Steffen Massberg, Hellen Ishikawa-Ankerhold, Bernd Engelmann

*These authors contributed equally to this study

8. Acknowledgement

Firstly, I would like kindly to express my sincere gratitude to my supervisor Prof. Dr. Roland Rad, and my mentor Prof. Dr. med Bernd Engelmann. Thanks for offering me a wonderful opportunity to work and learn in this state-of-the-art laboratory. They are both great scientists and unprecedented supervisors. They always guide me in directions when I had trouble with this project. Because of their unparalleled insights in basic research, they made tedious science full of fascinations and interest. They shed light on my whole project and they were always ready to help me to overcome difficulties in my life in Germany, especially during the pandemic. So many thanks should be given to Prof. Rad and Prof. Engelmann.

Secondly, I really appreciated support from my family and wife. Without their unwavering support, I could not have a chance to come to a new country to learn and experience another life, which is totally different from that in China.

Thirdly, I would like to acknowledge Prof. Steffen Massberg, Prof. Christian Schulz, and Dr. Kathrin Gärtner. With their permission, I could work in Webex and get to know lots of interesting colleagues there. This enriched not only my horizon in research but also my social life.

Last but not least, I would like to thank Dr. Zhe Zhang, Dr. Manovriti Thakur and doctoral candidate Mr. Michael Völkl, Mr. Junfu Luo, Mr. Marian Radev, Ms. Magda-Lena Berchtold, Ms. Esra Büyüközkan, Ms. Martina Reiser, Ms. Tonina Müller, Ms. Mona Wohlrab, for giving me the possibility to perform this promising project smoothly.

References

Abels, E. R. and X. O. Breakefield (2016). "Introduction to Extracellular Vesicles: Biogenesis, RNA Cargo Selection, Content, Release, and Uptake." Cell Mol Neurobiol **36**(3): 301-312.

Ahmad, S. A., W. B. Liu, Y. D. Jung, F. Fan and L. M. Ellis (2001). "The Effects of Angiopoietin-1 and -2 on Tumor Growth and Angiogenesis in Human Colon Cancer." Cancer Research **61**(4): 1255-1259.

Akashi, K., D. Traver, T. Miyamoto and I. L. Weissman (2000). "A clonogenic common myeloid progenitor that gives rise to all myeloid lineages." Nature **404**(6774): 193-197.

Alkim, C., D. Sakiz, H. Alkim, A. Livaoglu, T. Kendir, H. Demirsoy, L. Erdem, N. Akbayir and M. Sokmen (2012). "Thrombospondin-1 and VEGF in inflammatory bowel disease." Libyan J Med **7**.

Alves, B. E., S. A. Montalvao, F. J. Aranha, T. F. Siegl, C. A. Souza, I. Lorand-Metze, J. M. Annichino-Bizzacchi and E. V. De Paula (2010). "Imbalances in serum angiopoietin concentrations are early predictors of septic shock development in patients with post chemotherapy febrile neutropenia." BMC Infect Dis **10**: 143.

Andren-Sandberg, A., I. Lecander, G. Martinsson and B. Astedt (1992). "Peaks in plasma plasminogen activator inhibitor-1 concentration may explain thrombotic events in cases of pancreatic carcinoma." Cancer **69**(12): 2884-2887.

Anfray, C., A. Ummarino, F. T. Andon and P. Allavena (2019). "Current Strategies to Target Tumor-Associated-Macrophages to Improve Anti-Tumor Immune Responses." Cells **9**(1).

Ardito, C. M., B. M. Gruner, K. K. Takeuchi, C. Lubeseder-Martellato, N. Teichmann, P. K. Mazur, K. E. Delgiorno, E. S. Carpenter, C. J. Halbrook, J. C. Hall, D. Pal, T. Briel, A. Herner, M. Trajkovic-Arsic, B. Sipos, G. Y. Liou, P. Storz, N. R. Murray, D. W. Threadgill, M. Sibilia, M. K. Washington, C. L. Wilson, R. M. Schmid, E. W. Raines, H. C. Crawford and J. T. Siveke (2012). "EGF receptor is required for KRAS-induced pancreatic tumorigenesis." Cancer Cell **22**(3): 304-317.

Are, C., S. Chowdhury, H. Ahmad, A. Ravipati, T. Song, S. Shrikandhe and L. Smith (2016). "Predictive global trends in the incidence and mortality of pancreatic cancer based on geographic location, socio-economic status, and demographic shift." J Surg Oncol **114**(6): 736-742.

Bariety, M. (1967). "[Tribute to Armand Trousseau (14 October 1801-23 June 1867)]." Bull Acad Natl Med **151**(31): 627-635.

Becker, A., B. K. Thakur, J. M. Weiss, H. S. Kim, H. Peinado and D. Lyden (2016). "Extracellular Vesicles in Cancer: Cell-to-Cell Mediators of Metastasis." Cancer Cell **30**(6): 836-848.

Beckett, K., S. Monier, L. Palmer, C. Alexandre, H. Green, E. Bonneil, G. Raposo, P. Thibault, R. Le Borgne and J. P. Vincent (2013). "Drosophila S2 cells secrete wingless on exosome-like vesicles but the wingless gradient forms independently of exosomes." Traffic **14**(1): 82-96.

Bharat, A., A. C. McQuattie-Pimentel and G. R. S. Budinger (2017). "Non-classical monocytes in tissue injury and cancer." Oncotarget **8**(63): 106171-106172.

Buscail, L., B. Bournet and P. Cordelier (2020). "Role of oncogenic KRAS in the diagnosis, prognosis and treatment of pancreatic cancer." Nat Rev Gastroenterol Hepatol **17**(3): 153-168.

Butler, T. P. and P. M. Gullino (1975). "Quantitation of cell shedding into efferent blood of mammary adenocarcinoma." Cancer Res **35**(3): 512-516.

Campello, E., A. Ilich, P. Simioni and N. S. Key (2019). "The relationship between pancreatic cancer and hypercoagulability: a comprehensive review on epidemiological and biological issues." Br J Cancer **121**(5): 359-371.

Carmeliet, P. (2001). "Biomedicine. Clotting factors build blood vessels." Science **293**(5535): 1602-1604.

Chang, Y. S., E. di Tomaso, D. M. McDonald, R. Jones, R. K. Jain and L. L. Munn (2000). "Mosaic blood vessels in tumors: frequency of cancer cells in contact with flowing blood." Proc Natl Acad Sci U S A **97**(26): 14608-14613.

Chao, M. P., A. A. Alizadeh, C. Tang, J. H. Myklebust, B. Varghese, S. Gill, M. Jan, A. C. Cha, C. K. Chan, B. T. Tan, C. Y. Park, F. Zhao, H. E. Kohrt, R. Malumbres, J. Briones, R. D. Gascoyne, I. S. Lossos, R. Levy, I. L. Weissman and R. Majeti (2010). "Anti-CD47 antibody synergizes with rituximab to promote phagocytosis and eradicate non-Hodgkin lymphoma." Cell **142**(5): 699-713.

Chen, D. P., W. R. Ning, X. F. Li, Y. Wei, X. M. Lao, J. C. Wang, Y. Wu and L. Zheng (2018). "Peritumoral monocytes induce cancer cell autophagy to facilitate the progression of human hepatocellular carcinoma." Autophagy **14**(8): 1335-1346.

Cho, H., Y. Seo, K. M. Loke, S. W. Kim, S. M. Oh, J. H. Kim, J. Soh, H. S. Kim, H. Lee, J. Kim, J. J. Min, D. W. Jung and D. R. Williams (2018). "Cancer-Stimulated CAFs Enhance Monocyte Differentiation and Protumoral TAM Activation via IL6 and GM-CSF Secretion." Clin Cancer Res **24**(21): 5407-5421.

Cocucci, E., G. Racchetti and J. Meldolesi (2009). "Shedding microvesicles: artefacts no more." Trends Cell Biol **19**(2): 43-51.

Collaborators, G. B. D. P. C. (2019). "The global, regional, and national burden of pancreatic cancer and its attributable risk factors in 195 countries and territories, 1990-2017: a

systematic analysis for the Global Burden of Disease Study 2017." Lancet Gastroenterol Hepatol **4**(12): 934-947.

Collisson, E. A., C. L. Trejo, J. M. Silva, S. Gu, J. E. Korkola, L. M. Heiser, R. P. Charles, B. A. Rabinovich, B. Hann, D. Dankort, P. T. Spellman, W. A. Phillips, J. W. Gray and M. McMahon (2012). "A central role for RAF-->MEK-->ERK signaling in the genesis of pancreatic ductal adenocarcinoma." Cancer Discov **2**(8): 685-693.

Costa-Silva, B., N. M. Aiello, A. J. Ocean, S. Singh, H. Zhang, B. K. Thakur, A. Becker, A. Hoshino, M. T. Mark, H. Molina, J. Xiang, T. Zhang, T. M. Theilen, G. Garcia-Santos, C. Williams, Y. Ararso, Y. Huang, G. Rodrigues, T. L. Shen, K. J. Labori, I. M. Lothe, E. H. Kure, J. Hernandez, A. Doussot, S. H. Ebbesen, P. M. Grandgenett, M. A. Hollingsworth, M. Jain, K. Mallya, S. K. Batra, W. R. Jarnagin, R. E. Schwartz, I. Matei, H. Peinado, B. Z. Stanger, J. Bromberg and D. Lyden (2015). "Pancreatic cancer exosomes initiate pre-metastatic niche formation in the liver." Nat Cell Biol **17**(6): 816-826.

D'Amico, A. and L. Wu (2003). "The early progenitors of mouse dendritic cells and plasmacytoid predendritic cells are within the bone marrow hemopoietic precursors expressing Flt3." J Exp Med **198**(2): 293-303.

Dalton, A. J. (1975). "Microvesicles and vesicles of multivesicular bodies versus "virus-like" particles." J Natl Cancer Inst **54**(5): 1137-1148.

Daly, C., A. Eichten, C. Castanaro, E. Pasnikowski, A. Adler, A. S. Lalani, N. Papadopoulos, A. H. Kyle, A. I. Minchinton, G. D. Yancopoulos and G. Thurston (2013). "Angiopoietin-2 functions as a Tie2 agonist in tumor models, where it limits the effects of VEGF inhibition." Cancer Res **73**(1): 108-118.

Davis, S., N. Papadopoulos, T. H. Aldrich, P. C. Maisonpierre, T. Huang, L. Kovac, A. Xu, R. Leidich, E. Radziejewska, A. Rafique, J. Goldberg, V. Jain, K. Bailey, M. Karow, J. Fandl, S. J. Samuelsson, E. Ioffe, J. S. Rudge, T. J. Daly, C. Radziejewski and G. D. Yancopoulos (2003). "Angiopoietins have distinct modular domains essential for receptor binding, dimerization and superclustering." Nat Struct Biol **10**(1): 38-44.

Debien, E., K. Mayol, V. Biajoux, C. Daussy, M. G. De Aguero, M. Taillardet, N. Dagany, L. Brinza, T. Henry, B. Dubois, D. Kaiserlian, J. Marvel, K. Balabanian and T. Walzer (2013). "S1PR5 is pivotal for the homeostasis of patrolling monocytes." Eur J Immunol **43**(6): 1667-1675.

Desch, A., E. A. Strozyk, A. T. Bauer, V. Huck, V. Niemeyer, T. Wieland and S. W. Schneider (2012). "Highly invasive melanoma cells activate the vascular endothelium via an MMP-2/integrin αvβ5-induced secretion of VEGF-A." Am J Pathol **181**(2): 693-705.

Devalaraja, S., T. K. J. To, I. W. Folkert, R. Natesan, M. Z. Alam, M. Li, Y. Tada, K. Budagyan, M. T. Dang, L. Zhai, G. P. Lobel, G. E. Ciotti, T. S. K. Eisinger-Mathason, I. A. Asangani, K. Weber, M. C. Simon and M. Haldar (2020). "Tumor-Derived Retinoic Acid Regulates Intratumoral Monocyte Differentiation to Promote Immune Suppression." Cell **180**(6): 1098-1114 e1016.

Disease, G. B. D., I. Injury and C. Prevalence (2016). "Global, regional, and national incidence, prevalence, and years lived with disability for 310 diseases and injuries, 1990-2015: a systematic analysis for the Global Burden of Disease Study 2015." Lancet **388**(10053): 1545-1602.

Downward, J. (2003). "Targeting RAS signalling pathways in cancer therapy." Nat Rev Cancer **3**(1): 11-22.

Du, R., K. V. Lu, C. Petritsch, P. Liu, R. Ganss, E. Passegue, H. Song, S. Vandenberg, R. S. Johnson, Z. Werb and G. Bergers (2008). "HIF1alpha induces the recruitment of bone marrow-derived vascular modulatory cells to regulate tumor angiogenesis and invasion." Cancer Cell **13**(3): 206-220.

Ducreux, M., V. Boige and D. Malka (2007). "Treatment of advanced pancreatic cancer." Semin Oncol **34**(2 Suppl 1): S25-30.

Eitan, E., C. Suire, S. Zhang and M. P. Mattson (2016). "Impact of lysosome status on extracellular vesicle content and release." Ageing Res Rev **32**: 65-74.

Eser, S., N. Reiff, M. Messer, B. Seidler, K. Gottschalk, M. Dobler, M. Hieber, A. Arbeiter, S. Klein, B. Kong, C. W. Michalski, A. M. Schlitter, I. Esposito, A. J. Kind, L. Rad, A. E. Schnieke, M. Baccarini, D. R. Alessi, R. Rad, R. M. Schmid, G. Schneider and D. Saur (2013). "Selective requirement of PI3K/PDK1 signaling for Kras oncogene-driven pancreatic cell plasticity and cancer." Cancer Cell **23**(3): 406-420.

Etoh, T., H. Inoue, S. Tanaka, G. F. Barnard, S. Kitano and M. Mori (2001). "Angiopoietin-2 is related to tumor angiogenesis in gastric carcinoma: possible in vivo regulation via induction of proteases." Cancer Res **61**(5): 2145-2153.

Fabbri, M., A. Paone, F. Calore, R. Galli, E. Gaudio, R. Santhanam, F. Lovat, P. Fadda, C. Mao, G. J. Nuovo, N. Zanesi, M. Crawford, G. H. Ozer, D. Wernicke, H. Alder, M. A. Caligiuri, P. Nana-Sinkam, D. Perrotti and C. M. Croce (2012). "MicroRNAs bind to Toll-like receptors to induce prometastatic inflammatory response." Proc Natl Acad Sci U S A **109**(31): E2110-2116.

Feldmann, G., A. Mishra, S. M. Hong, S. Bisht, C. J. Strock, D. W. Ball, M. Goggins, A. Maitra and B. D. Nelkin (2010). "Inhibiting the cyclin-dependent kinase CDK5 blocks pancreatic cancer formation and progression through the suppression of Ras-Ral signaling." Cancer Res **70**(11): 4460-4469.

Fidler, I. J. (2003). "The pathogenesis of cancer metastasis: the 'seed and soil' hypothesis revisited." Nat Rev Cancer **3**(6): 453-458.

Fogg, D. K., C. Sibon, C. Miled, S. Jung, P. Aucouturier, D. R. Littman, A. Cumano and F. Geissmann (2006). "A clonogenic bone marrow progenitor specific for macrophages and dendritic cells." Science **311**(5757): 83-87.

Franklin, R. A., W. Liao, A. Sarkar, M. V. Kim, M. R. Bivona, K. Liu, E. G. Pamer and M. O. Li (2014). "The cellular and molecular origin of tumor-associated macrophages." Science **344**(6186): 921-925.

Geddings, J. E. and N. Mackman (2013). "Tumor-derived tissue factor-positive microparticles and venous thrombosis in cancer patients." Blood **122**(11): 1873-1880.

Geissmann, F., S. Jung and D. R. Littman (2003). "Blood monocytes consist of two principal subsets with distinct migratory properties." Immunity **19**(1): 71-82.

Goodsell, D. S. (1999). "The molecular perspective: the ras oncogene." Oncologist **4**(3): 263-264.

Gordon, I. O. and R. S. Freedman (2006). "Defective antitumor function of monocyte-derived macrophages from epithelial ovarian cancer patients." Clin Cancer Res **12**(5): 1515-1524.

Gouveia-Fernandes, S. (2020). "Monocytes and Macrophages in Cancer: Unsuspected Roles." Adv Exp Med Biol **1219**: 161-185.

Greco, V., M. Hannus and S. Eaton (2001). "Argosomes: a potential vehicle for the spread of morphogens through epithelia." Cell **106**(5): 633-645.

Gross, J. C., V. Chaudhary, K. Bartscherer and M. Boutros (2012). "Active Wnt proteins are secreted on exosomes." Nat Cell Biol **14**(10): 1036-1045.

Hanna, R. N., L. M. Carlin, H. G. Hubbeling, D. Nackiewicz, A. M. Green, J. A. Punt, F. Geissmann and C. C. Hedrick (2011). "The transcription factor NR4A1 (Nur77) controls bone marrow differentiation and the survival of Ly6C- monocytes." Nat Immunol **12**(8): 778-785.

Hanna, R. N., C. Cekic, D. Sag, R. Tacke, G. D. Thomas, H. Nowyhed, E. Herrley, N. Rasquinha, S. McArdle, R. Wu, E. Peluso, D. Metzger, H. Ichinose, I. Shaked, G. Chodaczek, S. K. Biswas and C. C. Hedrick (2015). "Patrolling monocytes control tumor metastasis to the lung." Science **350**(6263): 985-990.

Harvey, J. J. (1964). "An Unidentified Virus Which Causes the Rapid Production of Tumours in Mice." Nature **204**: 1104-1105.

Hawighorst, T., M. Skobe, M. Streit, Y. K. Hong, P. Velasco, L. F. Brown, L. Riccardi, B. Lange-Asschenfeldt and M. Detmar (2002). "Activation of the tie2 receptor by angiopoietin-1

enhances tumor vessel maturation and impairs squamous cell carcinoma growth." Am J Pathol **160**(4): 1381-1392.

Hayes, A. J., W. Q. Huang, J. Yu, P. C. Maisonpierre, A. Liu, F. G. Kern, M. E. Lippman, S. W. McLeskey and L. Y. Li (2000). "Expression and function of angiopoietin-1 in breast cancer." Br J Cancer **83**(9): 1154-1160.

Headley, M. B., A. Bins, A. Nip, E. W. Roberts, M. R. Looney, A. Gerard and M. F. Krummel (2016). "Visualization of immediate immune responses to pioneer metastatic cells in the lung." Nature **531**(7595): 513-517.

Hernandez, M. R., G. Escolar, J. Bozzo, A. M. Galan and A. Ordinas (1997). "Inhibition of fibrin deposition on the subendothelium by a monoclonal antibody to polymorphonuclear leukocyte integrin CD11b. Studies in a flow system." Haematologica **82**(5): 566-571.

Hettinger, J., D. M. Richards, J. Hansson, M. M. Barra, A. C. Joschko, J. Krijgsveld and M. Feuerer (2013). "Origin of monocytes and macrophages in a committed progenitor." Nat Immunol **14**(8): 821-830.

Himes, B. T., T. E. Peterson, T. de Mooij, L. M. C. Garcia, M. Y. Jung, S. Uhm, D. Yan, J. Tyson, H. J. Jin-Lee, D. Parney, Y. Abukhadra, M. P. Gustafson, A. B. Dietz, A. J. Johnson, H. Dong, R. L. Maus, S. Markovic, F. Lucien and I. F. Parney (2020). "The role of extracellular vesicles and PD-L1 in glioblastoma-mediated immunosuppressive monocyte induction." Neuro Oncol **22**(7): 967-978.

Hirayama, K., H. Kono, Y. Nakata, Y. Akazawa, H. Wakana, H. Fukushima and H. Fujii (2018). "Expression of podoplanin in stromal fibroblasts plays a pivotal role in the prognosis of patients with pancreatic cancer." Surg Today **48**(1): 110-118.

Hoshino, A., B. Costa-Silva, T. L. Shen, G. Rodrigues, A. Hashimoto, M. Tesic Mark, H. Molina, S. Kohsaka, A. Di Giannatale, S. Ceder, S. Singh, C. Williams, N. Soplop, K. Uryu, L. Pharmer, T. King, L. Bojmar, A. E. Davies, Y. Ararso, T. Zhang, H. Zhang, J. Hernandez, J. M. Weiss, V. D. Dumont-Cole, K. Kramer, L. H. Wexler, A. Narendran, G. K. Schwartz, J. H. Healey, P. Sandstrom, K. J. Labori, E. H. Kure, P. M. Grandgenett, M. A. Hollingsworth, M. de Sousa, S. Kaur, M. Jain, K. Mallya, S. K. Batra, W. R. Jarnagin, M. S. Brady, O. Fodstad, V. Muller, K. Pantel, A. J. Minn, M. J. Bissell, B. A. Garcia, Y. Kang, V. K. Rajasekhar, C. M. Ghajar, I. Matei, H. Peinado, J. Bromberg and D. Lyden (2015). "Tumour exosome integrins determine organotropic metastasis." Nature **527**(7578): 329-335.

Ikeda, O., H. Egami, T. Ishiko, S. Ishikawa, H. Kamohara, H. Hidaka, S. Mita and M. Ogawa (2003). "Expression of proteinase-activated receptor-2 in human pancreatic cancer: a possible relation to cancer invasion and induction of fibrosis." Int J Oncol **22**(2): 295-300.

Jaiswal, S., C. H. Jamieson, W. W. Pang, C. Y. Park, M. P. Chao, R. Majeti, D. Traver, N. van Rooijen and I. L. Weissman (2009). "CD47 is upregulated on circulating hematopoietic stem cells and leukemia cells to avoid phagocytosis." Cell **138**(2): 271-285.

Jakubzick, C., E. L. Gautier, S. L. Gibbings, D. K. Sojka, A. Schlitzer, T. E. Johnson, S. Ivanov, Q. Duan, S. Bala, T. Condon, N. van Rooijen, J. R. Grainger, Y. Belkaid, A. Ma'ayan, D. W. Riches, W. M. Yokoyama, F. Ginhoux, P. M. Henson and G. J. Randolph (2013). "Minimal differentiation of classical monocytes as they survey steady-state tissues and transport antigen to lymph nodes." Immunity **39**(3): 599-610.

Jarmalaviciute, A. and A. Pivoriunas (2016). "Exosomes as a potential novel therapeutic tools against neurodegenerative diseases." Pharmacol Res **113**(Pt B): 816-822.

Jeansson, M., A. Gawlik, G. Anderson, C. Li, D. Kerjaschki, M. Henkelman and S. E. Quaggin (2011). "Angiopoietin-1 is essential in mouse vasculature during development and in response to injury." J Clin Invest **121**(6): 2278-2289.

Jones, N., S. H. Chen, C. Sturk, Z. Master, J. Tran, R. S. Kerbel and D. J. Dumont (2003). "A unique autophosphorylation site on Tie2/Tek mediates Dok-R phosphotyrosine binding domain binding and function." Mol Cell Biol **23**(8): 2658-2668.

Jones, N., Z. Master, J. Jones, D. Bouchard, Y. Gunji, H. Sasaki, R. Daly, K. Alitalo and D. J. Dumont (1999). "Identification of Tek/Tie2 binding partners. Binding to a multifunctional docking site mediates cell survival and migration." J Biol Chem **274**(43): 30896-30905.

Kakkar, A. K., N. R. Lemoine, M. F. Scully, S. Tebbutt and R. C. Williamson (1995). "Tissue factor expression correlates with histological grade in human pancreatic cancer." Br J Surg **82**(8): 1101-1104.

Khorana, A. A. (2003). "Malignancy, thrombosis and Trousseau: the case for an eponym." J Thromb Haemost **1**(12): 2463-2465.

Kim, I., J. H. Kim, S. O. Moon, H. J. Kwak, N. G. Kim and G. Y. Koh (2000). "Angiopoietin-2 at high concentration can enhance endothelial cell survival through the phosphatidylinositol 3'-kinase/Akt signal transduction pathway." Oncogene **19**(39): 4549-4552.

Kim, K. T., H. H. Choi, M. O. Steinmetz, B. Maco, R. A. Kammerer, S. Y. Ahn, H. Z. Kim, G. M. Lee and G. Y. Koh (2005). "Oligomerization and multimerization are critical for angiopoietin-1 to bind and phosphorylate Tie2." J Biol Chem **280**(20): 20126-20131.

Klein, C. A. (2008). "Cancer. The metastasis cascade." Science **321**(5897): 1785-1787.

Kopytek, M., M. Zabczyk, J. Natorska, J. Siudut, K. P. Malinowski, P. Ptaszek, A. Glajcar, T. Goralczyk and A. Undas (2019). "Viscoelastic properties of plasma fibrin clots are similar in patients on rivaroxaban and vitamin K antagonists." J Physiol Pharmacol **70**(1).

Krishnan, H., J. Rayes, T. Miyashita, G. Ishii, E. P. Retzbach, S. A. Sheehan, A. Takemoto, Y. W. Chang, K. Yoneda, J. Asai, L. Jensen, L. Chalise, A. Natsume and G. S. Goldberg (2018). "Podoplanin: An emerging cancer biomarker and therapeutic target." Cancer Sci **109**(5): 1292-1299.

Kubo, H., S. Mensurado, N. Goncalves-Sousa, K. Serre and B. Silva-Santos (2017). "Primary Tumors Limit Metastasis Formation through Induction of IL15-Mediated Cross-Talk between Patrolling Monocytes and NK Cells." Cancer Immunol Res **5**(9): 812-820.

Kucharzewska, P., H. C. Christianson, J. E. Welch, K. J. Svensson, E. Fredlund, M. Ringner, M. Morgelin, E. Bourseau-Guilmain, J. Bengzon and M. Belting (2013). "Exosomes reflect the hypoxic status of glioma cells and mediate hypoxia-dependent activation of vascular cells during tumor development." Proc Natl Acad Sci U S A **110**(18): 7312-7317.

Lavin, Y., S. Kobayashi, A. Leader, E. D. Amir, N. Elefant, C. Bigenwald, R. Remark, R. Sweeney, C. D. Becker, J. H. Levine, K. Meinhof, A. Chow, S. Kim-Shulze, A. Wolf, C. Medaglia, H. Li, J. A. Rytlewski, R. O. Emerson, A. Solovyov, B. D. Greenbaum, C. Sanders, M. Vignali, M. B. Beasley, R. Flores, S. Gnjatic, D. Pe'er, A. Rahman, I. Amit and M. Merad (2017). "Innate Immune Landscape in Early Lung Adenocarcinoma by Paired Single-Cell Analyses." Cell **169**(4): 750-765 e717.

Lim, K. H., A. T. Baines, J. J. Fiordalisi, M. Shipitsin, L. A. Feig, A. D. Cox, C. J. Der and C. M. Counter (2005). "Activation of RalA is critical for Ras-induced tumorigenesis of human cells." Cancer Cell **7**(6): 533-545.

Lopez-Verrilli, M. A., F. Picou and F. A. Court (2013). "Schwann cell-derived exosomes enhance axonal regeneration in the peripheral nervous system." Glia **61**(11): 1795-1806.

Lu, P., V. M. Weaver and Z. Werb (2012). "The extracellular matrix: a dynamic niche in cancer progression." J Cell Biol **196**(4): 395-406.

Lurje, I., L. Hammerich and F. Tacke (2020). "Dendritic Cell and T Cell Crosstalk in Liver Fibrogenesis and Hepatocarcinogenesis: Implications for Prevention and Therapy of Liver Cancer." Int J Mol Sci **21**(19).

Maas, S. L. N., X. O. Breakefield and A. M. Weaver (2017). "Extracellular Vesicles: Unique Intercellular Delivery Vehicles." Trends Cell Biol **27**(3): 172-188.

Maheswaran, S. and D. A. Haber (2010). "Circulating tumor cells: a window into cancer biology and metastasis." Curr Opin Genet Dev **20**(1): 96-99.

Maisonpierre, P. C., C. Suri, P. F. Jones, S. Bartunkova, S. J. Wiegand, C. Radziejewski, D. Compton, J. McClain, T. H. Aldrich, N. Papadopoulos, T. J. Daly, S. Davis, T. N. Sato and G. D.

Yancopoulos (1997). "Angiopoietin-2, a natural antagonist for Tie2 that disrupts in vivo angiogenesis." Science **277**(5322): 55-60.

Malumbres, M. and M. Barbacid (2003). "RAS oncogenes: the first 30 years." Nat Rev Cancer **3**(6): 459-465.

Mezouar, S., C. Frere, R. Darbousset, D. Mege, L. Crescence, F. Dignat-George, L. Panicot-Dubois and C. Dubois (2016). "Role of platelets in cancer and cancer-associated thrombosis: Experimental and clinical evidences." Thromb Res **139**: 65-76.

Miller, K. D., L. Nogueira, A. B. Mariotto, J. H. Rowland, K. R. Yabroff, C. M. Alfano, A. Jemal, J. L. Kramer and R. L. Siegel (2019). "Cancer treatment and survivorship statistics, 2019." CA Cancer J Clin **69**(5): 363-385.

Minciacchi, V. R., M. R. Freeman and D. Di Vizio (2015). "Extracellular vesicles in cancer: exosomes, microvesicles and the emerging role of large oncosomes." Semin Cell Dev Biol **40**: 41-51.

Molina-Arcas, M., D. C. Hancock, C. Sheridan, M. S. Kumar and J. Downward (2013). "Coordinate direct input of both KRAS and IGF1 receptor to activation of PI3 kinase in KRAS-mutant lung cancer." Cancer Discov **3**(5): 548-563.

Mueck, W., J. Stampfuss, D. Kubitza and M. Becka (2014). "Clinical pharmacokinetic and pharmacodynamic profile of rivaroxaban." Clin Pharmacokinet **53**(1): 1-16.

Mueller, S., T. Engleitner, R. Maresch, M. Zukowska, S. Lange, T. Kaltenbacher, B. Konukiewitz, R. Ollinger, M. Zwiebel, A. Strong, H. Y. Yen, R. Banerjee, S. Louzada, B. Fu, B. Seidler, J. Gotzfried, K. Schuck, Z. Hassan, A. Arbeiter, N. Schonhuber, S. Klein, C. Veltkamp, M. Friedrich, L. Rad, M. Barenboim, C. Ziegenhain, J. Hess, O. M. Dovey, S. Eser, S. Parekh, F. Constantino-Casas, J. de la Rosa, M. I. Sierra, M. Fraga, J. Mayerle, G. Kloppel, J. Cadinanos, P. Liu, G. Vassiliou, W. Weichert, K. Steiger, W. Enard, R. M. Schmid, F. Yang, K. Unger, G. Schneider, I. Varela, A. Bradley, D. Saur and R. Rad (2018). "Evolutionary routes and KRAS dosage define pancreatic cancer phenotypes." Nature **554**(7690): 62-68.

Murray, E. G. D., R. A. Webb and M. B. R. Swann (1926). "A disease of rabbits characterised by a large mononuclear leucocytosis, caused by a hitherto undescribed bacillus Bacterium monocytogenes (n.sp.)." The Journal of Pathology and Bacteriology **29**(4): 407-439.

Nabhan, J. F., R. Hu, R. S. Oh, S. N. Cohen and Q. Lu (2012). "Formation and release of arrestin domain-containing protein 1-mediated microvesicles (ARMMs) at plasma membrane by recruitment of TSG101 protein." Proc Natl Acad Sci U S A **109**(11): 4146-4151.

Nadir, Y. (2020). "Heparanase in the Coagulation System." Adv Exp Med Biol **1221**: 771-784.

Nadir, Y. and B. Brenner (2016). "Heparanase procoagulant activity in cancer progression." Thromb Res **140 Suppl 1**: S44-48.

Navas, C., I. Hernandez-Porras, A. J. Schuhmacher, M. Sibilia, C. Guerra and M. Barbacid (2012). "EGF receptor signaling is essential for k-ras oncogene-driven pancreatic ductal adenocarcinoma." Cancer Cell **22**(3): 318-330.

Neoptolemos, J. P., J. Kleeff, P. Michl, E. Costello, W. Greenhalf and D. H. Palmer (2018). "Therapeutic developments in pancreatic cancer: current and future perspectives." Nat Rev Gastroenterol Hepatol **15**(6): 333-348.

Oh, H., H. Takagi, K. Suzuma, A. Otani, M. Matsumura and Y. Honda (1999). "Hypoxia and vascular endothelial growth factor selectively up-regulate angiopoietin-2 in bovine microvascular endothelial cells." J Biol Chem **274**(22): 15732-15739.

Olingy, C. E., H. Q. Dinh and C. C. Hedrick (2019). "Monocyte heterogeneity and functions in cancer." J Leukoc Biol **106**(2): 309-322.

Ozdemir, T., P. Zhang, C. Fu and C. Dong (2012). "Fibrin serves as a divalent ligand that regulates neutrophil-mediated melanoma cells adhesion to endothelium under shear conditions." Am J Physiol Cell Physiol **302**(8): C1189-1201.

Patel, A. A., Y. Zhang, J. N. Fullerton, L. Boelen, A. Rongvaux, A. A. Maini, V. Bigley, R. A. Flavell, D. W. Gilroy, B. Asquith, D. Macallan and S. Yona (2017). "The fate and lifespan of human monocyte subsets in steady state and systemic inflammation." J Exp Med **214**(7): 1913-1923.

Perez, R. L. and J. Roman (1995). "Fibrin enhances the expression of IL-1 beta by human peripheral blood mononuclear cells. Implications in pulmonary inflammation." J Immunol **154**(4): 1879-1887.

Pfeiler, S., M. Thakur, P. Grunauer, R. T. A. Megens, U. Joshi, R. Coletti, V. Samara, G. Muller-Stoy, H. Ishikawa-Ankerhold, K. Stark, A. Klingl, T. Frohlich, G. J. Arnold, S. Wormann, C. J. Bruns, H. Algul, C. Weber, S. Massberg and B. Engelmann (2019). "CD36-triggered cell invasion and persistent tissue colonization by tumor microvesicles during metastasis." FASEB J **33**(2): 1860-1872.

Phinney, D. G., M. Di Giuseppe, J. Njah, E. Sala, S. Shiva, C. M. St Croix, D. B. Stolz, S. C. Watkins, Y. P. Di, G. D. Leikauf, J. Kolls, D. W. Riches, G. Deiuliis, N. Kaminski, S. V. Boregowda, D. H. McKenna and L. A. Ortiz (2015). "Mesenchymal stem cells use extracellular vesicles to outsource mitophagy and shuttle microRNAs." Nat Commun **6**: 8472.

Pishvaian, M. J. and J. R. Brody (2017). "Therapeutic Implications of Molecular Subtyping for Pancreatic Cancer." Oncology (Williston Park) **31**(3): 159-166, 168.

Plebanek, M. P., N. L. Angeloni, E. Vinokour, J. Li, A. Henkin, D. Martinez-Marin, S. Filleur, R. Bhowmick, J. Henkin, S. D. Miller, I. Ifergan, Y. Lee, I. Osman, C. S. Thaxton and O. V. Volpert (2017). "Pre-metastatic cancer exosomes induce immune surveillance by patrolling monocytes at the metastatic niche." Nat Commun **8**(1): 1319.

Prabowo, S. A., H. Painter, A. Zelmer, S. G. Smith, K. Seifert, M. Amat, P. J. Cardona and H. A. Fletcher (2019). "RUTI Vaccination Enhances Inhibition of Mycobacterial Growth ex vivo and Induces a Shift of Monocyte Phenotype in Mice." Front Immunol **10**: 894.

Rahib, L., B. D. Smith, R. Aizenberg, A. B. Rosenzweig, J. M. Fleshman and L. M. Matrisian (2014). "Projecting cancer incidence and deaths to 2030: the unexpected burden of thyroid, liver, and pancreas cancers in the United States." Cancer Res **74**(11): 2913-2921.

Ren, K., S. Li, J. Ding, S. Zhao, S. Liang, X. Cao, C. Su and J. Guo (2021). "Ginsenoside Rd attenuates mouse experimental autoimmune neuritis by modulating monocyte subsets conversion." Biomed Pharmacother **138**: 111489.

Rilla, K., H. Siiskonen, M. Tammi and R. Tammi (2014). "Hyaluronan-coated extracellular vesicles--a novel link between hyaluronan and cancer." Adv Cancer Res **123**: 121-148.

Robinson, A., C. Z. Han, C. K. Glass and J. W. Pollard (2021). "Monocyte Regulation in Homeostasis and Malignancy." Trends Immunol **42**(2): 104-119.

Ryan, D. P., T. S. Hong and N. Bardeesy (2014). "Pancreatic adenocarcinoma." N Engl J Med **371**(11): 1039-1049.

Ryu, J. K., M. A. Petersen, S. G. Murray, K. M. Baeten, A. Meyer-Franke, J. P. Chan, E. Vagena, C. Bedard, M. R. Machado, P. E. Rios Coronado, T. Prod'homme, I. F. Charo, H. Lassmann, J. L. Degen, S. S. Zamvil and K. Akassoglou (2015). "Blood coagulation protein fibrinogen promotes autoimmunity and demyelination via chemokine release and antigen presentation." Nat Commun **6**: 8164.

Sahni, A., C. A. Baker, L. A. Sporn and C. W. Francis (2000). "Fibrinogen and fibrin protect fibroblast growth factor-2 from proteolytic degradation." Thromb Haemost **83**(5): 736-741.

Schmid, M. C., S. Q. Khan, M. M. Kaneda, P. Pathria, R. Shepard, T. L. Louis, S. Anand, G. Woo, C. Leem, M. H. Faridi, T. Geraghty, A. Rajagopalan, S. Gupta, M. Ahmed, R. I. Vazquez-Padron, D. A. Cheresh, V. Gupta and J. A. Varner (2018). "Integrin CD11b activation drives anti-tumor innate immunity." Nat Commun **9**(1): 5379.

Serbina, N. V. and E. G. Pamer (2006). "Monocyte emigration from bone marrow during bacterial infection requires signals mediated by chemokine receptor CCR2." Nat Immunol **7**(3): 311-317.

Shigemori, C., H. Wada, K. Matsumoto, H. Shiku, S. Nakamura and H. Suzuki (1998). "Tissue factor expression and metastatic potential of colorectal cancer." Thromb Haemost **80**(6): 894-898.

Shim, W. S., I. A. Ho and P. E. Wong (2007). "Angiopoietin: a TIE(d) balance in tumor angiogenesis." Mol Cancer Res **5**(7): 655-665.

Siegel, R. L., K. D. Miller and A. Jemal (2020). "Cancer statistics, 2020." CA Cancer J Clin **70**(1): 7-30.

Skog, J., T. Wurdinger, S. van Rijn, D. H. Meijer, L. Gainche, M. Sena-Esteves, W. T. Curry, Jr., B. S. Carter, A. M. Krichevsky and X. O. Breakefield (2008). "Glioblastoma microvesicles transport RNA and proteins that promote tumour growth and provide diagnostic biomarkers." Nat Cell Biol **10**(12): 1470-1476.

Smiley, S. T., J. A. King and W. W. Hancock (2001). "Fibrinogen stimulates macrophage chemokine secretion through toll-like receptor 4." J Immunol **167**(5): 2887-2894.

Smith, R. A., K. S. Andrews, D. Brooks, S. A. Fedewa, D. Manassaram-Baptiste, D. Saslow and R. C. Wender (2019). "Cancer screening in the United States, 2019: A review of current American Cancer Society guidelines and current issues in cancer screening." CA Cancer J Clin **69**(3): 184-210.

Sprangers, S., T. J. de Vries and V. Everts (2016). "Monocyte Heterogeneity: Consequences for Monocyte-Derived Immune Cells." J Immunol Res **2016**: 1475435.

Sproul, E. E. (1938). "Carcinoma and Venous Thrombosis: The Frequency of Association of Carcinoma in the Body or Tail of the Pancreas with Multiple Venous Thrombosis." The American Journal of Cancer **34**(4): 566-585.

Stoeltzing, O., S. A. Ahmad, W. Liu, M. F. McCarty, J. S. Wey, A. A. Parikh, F. Fan, N. Reinmuth, M. Kawaguchi, C. D. Bucana and L. M. Ellis (2003). "Angiopoietin-1 inhibits vascular permeability, angiogenesis, and growth of hepatic colon cancer tumors." Cancer Res **63**(12): 3370-3377.

Suri, C., P. F. Jones, S. Patan, S. Bartunkova, P. C. Maisonpierre, S. Davis, T. N. Sato and G. D. Yancopoulos (1996). "Requisite role of angiopoietin-1, a ligand for the TIE2 receptor, during embryonic angiogenesis." Cell **87**(7): 1171-1180.

Tanaka, S., M. Mori, Y. Sakamoto, M. Makuuchi, K. Sugimachi and J. R. Wands (1999). "Biologic significance of angiopoietin-2 expression in human hepatocellular carcinoma." J Clin Invest **103**(3): 341-345.

Tesselaar, M. E., F. P. Romijn, I. K. Van Der Linden, F. A. Prins, R. M. Bertina and S. Osanto (2007). "Microparticle-associated tissue factor activity: a link between cancer and thrombosis?" J Thromb Haemost **5**(3): 520-527.

Thomas, G. D., R. N. Hanna, N. T. Vasudevan, A. A. Hamers, C. E. Romanoski, S. McArdle, K. D. Ross, A. Blatchley, D. Yoakum, B. A. Hamilton, Z. Mikulski, M. K. Jain, C. K. Glass and C. C. Hedrick (2016). "Deleting an Nr4a1 Super-Enhancer Subdomain Ablates Ly6C(low) Monocytes while Preserving Macrophage Gene Function." Immunity **45**(5): 975-987.

Tkach, M. and C. Thery (2016). "Communication by Extracellular Vesicles: Where We Are and Where We Need to Go." Cell **164**(6): 1226-1232.

Ueno, T., M. Toi, M. Koike, S. Nakamura and T. Tominaga (2000). "Tissue factor expression in breast cancer tissues: its correlation with prognosis and plasma concentration." Br J Cancer **83**(2): 164-170.

van Furth, R. and Z. A. Cohn (1968). "The origin and kinetics of mononuclear phagocytes." J Exp Med **128**(3): 415-435.

van Furth, R., Z. A. Cohn, J. G. Hirsch, J. H. Humphrey, W. G. Spector and H. L. Langevoort (1972). "The mononuclear phagocyte system: a new classification of macrophages, monocytes, and their precursor cells." Bull World Health Organ **46**(6): 845-852.

Wang, Y., A. Sang, M. Zhu, G. Zhang, H. Guan, M. Ji and H. Chen (2016). "Tissue factor induces VEGF expression via activation of the Wnt/beta-catenin signaling pathway in ARPE-19 cells." Mol Vis **22**: 886-897.

Willingham, S. B., J. P. Volkmer, A. J. Gentles, D. Sahoo, P. Dalerba, S. S. Mitra, J. Wang, H. Contreras-Trujillo, R. Martin, J. D. Cohen, P. Lovelace, F. A. Scheeren, M. P. Chao, K. Weiskopf, C. Tang, A. K. Volkmer, T. J. Naik, T. A. Storm, A. R. Mosley, B. Edris, S. M. Schmid, C. K. Sun, M. S. Chua, O. Murillo, P. Rajendran, A. C. Cha, R. K. Chin, D. Kim, M. Adorno, T. Raveh, D. Tseng, S. Jaiswal, P. O. Enger, G. K. Steinberg, G. Li, S. K. So, R. Majeti, G. R. Harsh, M. van de Rijn, N. N. Teng, J. B. Sunwoo, A. A. Alizadeh, M. F. Clarke and I. L. Weissman (2012). "The CD47-signal regulatory protein alpha (SIRPa) interaction is a therapeutic target for human solid tumors." Proc Natl Acad Sci U S A **109**(17): 6662-6667.

Wolf, P. (1967). "The nature and significance of platelet products in human plasma." Br J Haematol **13**(3): 269-288.

Wong, C. W., A. Lee, L. Shientag, J. Yu, Y. Dong, G. Kao, A. B. Al-Mehdi, E. J. Bernhard and R. J. Muschel (2001). "Apoptosis: an early event in metastatic inefficiency." Cancer Res **61**(1): 333-338.

Yao, J. L., C. K. Ryan, C. W. Francis, M. Kohli, M. B. Taubman and A. A. Khorana (2009). "Tissue factor and VEGF expression in prostate carcinoma: a tissue microarray study." Cancer Invest **27**(4): 430-434.

Yeap, W. H., K. L. Wong, N. Shimasaki, E. C. Teo, J. K. Quek, H. X. Yong, C. P. Diong, A. Bertoletti, Y. C. Linn and S. C. Wong (2017). "Corrigendum: CD16 is indispensable for antibody-dependent cellular cytotoxicity by human monocytes." Sci Rep **7**: 46202.

Yona, S. and S. Jung (2010). "Monocytes: subsets, origins, fates and functions." Curr Opin Hematol **17**(1): 53-59.

Yona, S., K. W. Kim, Y. Wolf, A. Mildner, D. Varol, M. Breker, D. Strauss-Ayali, S. Viukov, M. Guilliams, A. Misharin, D. A. Hume, H. Perlman, B. Malissen, E. Zelzer and S. Jung (2013). "Fate mapping reveals origins and dynamics of monocytes and tissue macrophages under homeostasis." Immunity **38**(1): 79-91.

Yuan, H. T., E. V. Khankin, S. A. Karumanchi and S. M. Parikh (2009). "Angiopoietin 2 is a partial agonist/antagonist of Tie2 signaling in the endothelium." Mol Cell Biol **29**(8): 2011-2022.

Zhang, J., C. Yin, Q. Zhao, Z. Zhao, J. Wang, R. J. Miron and Y. Zhang (2020). "Anti-inflammation effects of injectable platelet-rich fibrin via macrophages and dendritic cells." J Biomed Mater Res A **108**(1): 61-68.

Zhang, P., T. Ozdemir, C. Y. Chung, G. P. Robertson and C. Dong (2011). "Sequential binding of αVβ3 and ICAM-1 determines fibrin-mediated melanoma capture and stable adhesion to CD11b/CD18 on neutrophils." J Immunol **186**(1): 242-254.

Zhang, X. (2020). "Role of Blood Coagulation and Extracellular Vesicles in Pancreatic Cancer Cell Extravasation."

Zhang, X. (2020). Role of blood coagulation and extracellular vesicles in pancreatic cancer cell extravasation, LMU München.

Zhang, Y., Y. Deng, T. Luther, M. Muller, R. Ziegler, R. Waldherr, D. M. Stern and P. P. Nawroth (1994). "Tissue factor controls the balance of angiogenic and antiangiogenic properties of tumor cells in mice." J Clin Invest **94**(3): 1320-1327.

Ziegler-Heitbrock, L., P. Ancuta, S. Crowe, M. Dalod, V. Grau, D. N. Hart, P. J. Leenen, Y. J. Liu, G. MacPherson, G. J. Randolph, J. Scherberich, J. Schmitz, K. Shortman, S. Sozzani, H. Strobl, M. Zembala, J. M. Austyn and M. B. Lutz (2010). "Nomenclature of monocytes and dendritic cells in blood." Blood **116**(16): e74-80.

Affidavit – Ehrenwörtliche Erklärung

„Ich versichere, dass ich die vorliegende Arbeit ohne Hilfe Dritter und ohne Benutzung anderer als der angegebenen Quellen und Hilfsmittel angefertigt und die den benutzten Quellen wörtlich oder inhaltlich entnommenen Stellen als solche kenntlich gemacht habe. Diese Arbeit hat in gleicher oder ähnlicher Form noch keiner Prüfungsbehörde vorgelegen. Ich bin damit einverstanden, dass meine Arbeit zum Zwecke eines Plagiatsabgleichs in elektronischer Form anonymisiert versendet und gespeichert werden kann."

"I affirm that this thesis was written by myself without any unauthorized third-party support. All used references and resources are clearly indicated. All quotes and citations are properly referenced. This thesis was never presented in the past in the same or similar form to any examination board. I agree that my thesis may be subjected to electronic plagiarism check. For this purpose, an anonymous copy may be distributed and uploaded to servers within and outside the Technische Universität München."

München, 20.06.2021 (Signature)